Accepted Manuscript

Syntheses and *in vitro* evaluation of new S1PR1 compounds and initial evaluation of a lead F-18 radiotracer in rodents

Zonghua Luo, Adam J. Rosenberg, Hui Liu, Junbin Han, Zhude Tu

Please cite this article as: Z. Luo, A.J. Rosenberg, H. Liu, J. Han, Z. Tu, Syntheses and *in vitro* evaluation of new S1PR1 compounds and initial evaluation of a lead F-18 radiotracer in rodents, *European Journal of Medicinal Chemistry* (2018), doi: 10.1016/j.ejmech.2018.03.035.
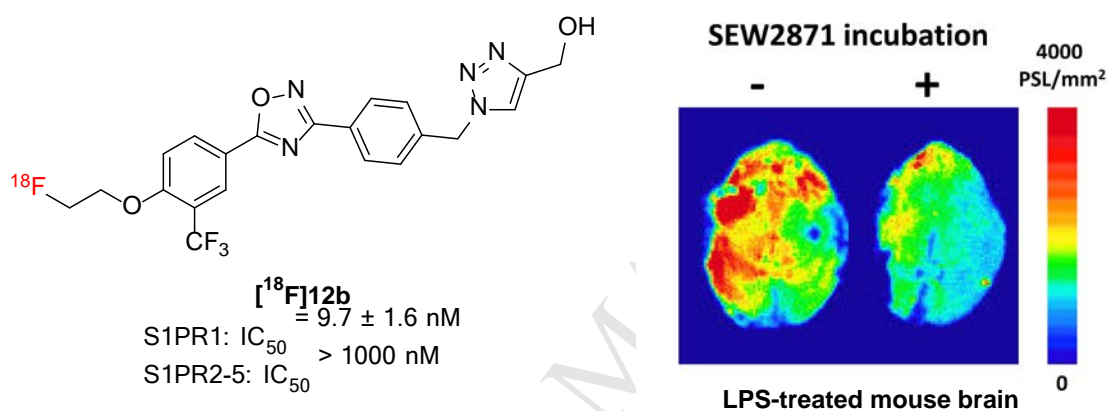
Graphical abstract

Syntheses and *in vitro* evaluation of new S1PR1 compounds and initial evaluation of a lead F-18 radiotracer in rodents

Zonghua Luo, Adam J. Rosenberg, Hui Liu, Junbin Han, and Zhude Tu*

Department of Radiology, Washington University School of Medicine, St. Louis, MO 63110, USA

[^{18}F]12b

S1PR1: IC_{50} = 9.7 ± 1.6 nM
S1PR2-5: IC_{50} > 1000 nM

SEW2871 incubation

LPS-treated mouse brain

Syntheses and *in vitro* evaluation of new S1PR1 compounds and initial evaluation of

a lead F-18 radiotracer in rodents

Zonghua Luo, Adam J. Rosenberg, Hui Liu, Junbin Han, and Zhude Tu*

Department of Radiology, Washington University School of Medicine, St. Louis, MO 63110, USA

Total Pages: 33

Schemes: 5

Tables: 3

Figures: 5

*Address correspondence to:

Zhude Tu, Ph.D.

Department of Radiology

Washington University School of Medicine

Campus Box 8225

510 S. Kingshighway Blvd.

St. Louis, MO 63110, USA

Tel: 1-314-362-8487

Fax: 1-314-362-8555

E-mail: zhudetu@wustl.edu

Abstract

Thirteen new S1PR1 ligands were designed and synthesized by replacing azetidine-3-carboxylic acid moiety of compound **4** with new polar groups. The *in vitro* binding potency of these new analogs toward S1PR1 was

determined. Out of 13 new compounds, four compounds **9a**, **10c**, **12b**, and **16b** displayed high S1PR1 binding potency with IC_{50} values of 13.2 ± 3.2, 14.7 ± 1.7, 9.7 ± 1.6, and 6.3 ± 1.3 nM, respectively; further binding studies of these four ligands toward S1PR2-5 suggested they are highly selective for S1PR1 over other S1PRs. The radiosynthesis of the lead radiotracer [^{18}F]**12b** was achieved with good radiochemical yield (~14.1%), high radiochemical purity (> 98%), and good specific activity (~54.1 GBq/µmol, decay corrected to the end of synthesis, EOS). *Ex vivo* autoradiography and initial biodistribution studies in rodents were performed, suggesting that [^{18}F]**12b** was able to penetrate the blood-brain barrier (BBB) with high brain uptake (0.71% ID/g at 60 min post injection) and no defluorination was observed. *In vitro* autoradiography study in brain slices of lipopolysaccharides (LPS)-induced neuroinflammation mice indicated that SEW2871, a specific S1PR1 ligand was able to reduce the uptake of [^{18}F]**12b**, suggesting [^{18}F]**12b** has S1PR1 specific binding. These initial results suggested that [^{18}F]**12b** has potential to be a F-18 labeled radiotracer for imaging S1PR1 in the brain of the animal *in vivo*.

Key words: Sphingosine-1-phosphate receptor 1; F-18 radiotracer; PET; Multiple sclerosis; Autoradiography; Biodistribution.

1. Introduction

Sphingosine-1-phosphate receptor 1 (S1PR1) is a G-protein-coupled receptor which is widely expressed in different cells such as immune cells, neural cells, endothelial cells, and smooth muscle cells. Acting with the naturally occurring lipid mediator molecule sphingosine 1-phosphate (S1P, Fig. 1), S1PR1 initiates signaling cascades that exert various biological functions, such as cell survival and differentiation, inflammation, cardiovascular function, and vascular permeability [1]. It was reported that S1P/S1PR1 signaling system plays a key role in immune-mediated diseases, such as multiple sclerosis (MS) [2, 3], colitis [4], influenza [5], rheumatoid arthritis [6], inflammatory bowel disease [7], and atherosclerosis [8, 9]. In MS, S1PR1 involves in immune-cell trafficking and activation, astrocyte proliferation, microglia activation, and interruption of the BBB function [10, 11]. Fingolimod (FTY720, Fig. 1), an S1PR modulator, is the first oral drug that US Food and Drug Administration (FDA) approved for treating remitting-relapsing MS [11]. *In vivo,* FTY720 is

phosphorylated to form a bioactive metabolite, FTY720-P that exerts its disease-ameliorating effects by down-modulation of S1PR1 expression from the cell surface and altering lymphocyte trafficking [10]. Currently, targeting on S1PR1 represents a novel therapeutic strategy for MS and other inflammatory diseases.
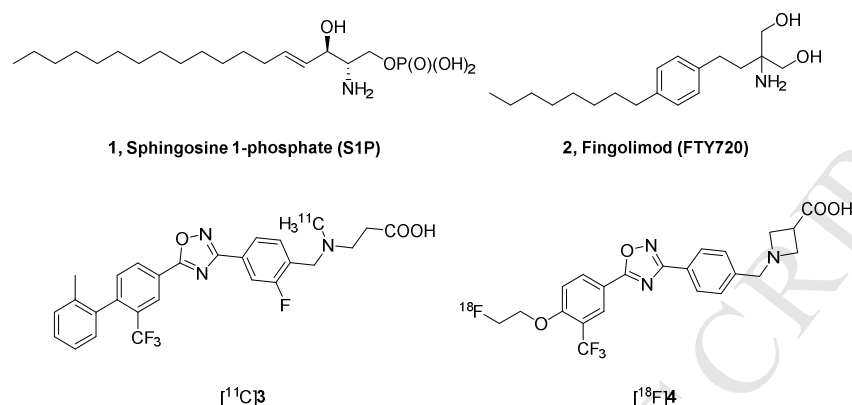

Fig. 1. Structure of S1P, FTY720, and S1PR1 PET tracers.

Positron emission tomography (PET) provides a unique noninvasive imaging tool for quantitative assessment of target protein *in vivo* and it is used widely in preclinical and clinical investigations of assessing receptor occupancy, downstream functional changes, and diseases pathophysiology for guiding drug development [12]. Using a specific S1PR1 radiotracer, PET could advance our understanding of the S1PR1 pathophysiologic functions in diseases. Utilizing a specific C-11 labeled S1PR1 radiotracer [^{11}C]**3** (Fig. 1), we reported the feasibility of imaging measure S1PR1 expression for its inflammatory response in three animal models of diseases, the experimental autoimmune encephalomyelitis (EAE) rat model of MS [13], the femoral artery wire-injury mouse model of neointimal hyperplasia [14], and the carotid artery balloon injury rat model of vascular inflammation [15]. Because F-18 isotope has a longer half-life ($t_{1/2}$ = 109.8 min) than C-11 ($t_{1/2}$ = 20.4 min), F-18 tracers provide additional advantages of fewer constraints for production, delivery to satellite clinical PET sites with 3-4 hours' drive distance, permission of longer scan sessions, and higher target-to-reference ratios. Therefore, identification of a F-18 radiotracer for imaging S1PR1 *in vivo* is imperative in PET community. To develop F-18 labeled S1PR1 radiotracers, Haufe's group firstly reported three ^{18}F-labeled FTY-720 analogs as S1PR radiotracers [16, 17]. These F-18 labeled radiotracers were evaluated in rodents with PET imaging modality for their inflammation responses by assessing S1PR1 expression at the binding sites. However, *in vivo* defluorination and low selectivity of these radiotracers prevented further transferring these

radiotracers into clinical evaluation. Recently, we reported our *in vivo* investigation of a selective F-18 S1PR1 tracer [^{18}F]**4** for its response to acute liver inflammation of rat model that was induced by injection of LPS [18]. Although it showed positive response in liver inflammation, [^{18}F]**4** is unable to penetrate the BBB, preventing its implementation in the assessment of neuroinflammation *in vivo*. To overcome this limitation, herein, we reported our efforts on design, syntheses, and *in vitro* bioactivity evaluation of 13 new analogs; among these 13 new analogs, the F-18 labeled [^{18}F]**12b** was further radiosynthesized and performed initial evaluation to check its specificity and capability of penetrating the BBB in rodents *in vivo*.

## 2. Results and discussion

2.1. *Chemistry*

Generally, the S1PR1 compound structure is composed of a lipophilic terminal group that interacts with the hydrophobic binding pocket of S1PR1, a polar head group, and a rigid aryl or heteroaryl linker. Generally, optimization of using a carboxylic acid as the polar head group lead to discovering high potent and highly selective S1PR1 agonists [19]. The promising *in vitro* binding data of compound **4** that has an aryl azetidine carboxylic acid group [18] encourages us to further optimize the aryl azetidine carboxylic acid group using other hydrophilic groups to identify new analogs having improved binding properties and physicochemical properties. In current work, we replaced the aryl azetidine carboxyl acid group with aryl sulfonamide, amide, *N*-hydroxy amide, hydrazide, alcohol, carboxyl acid, and amine groups to generate new analogs. The syntheses of these new analogs were illustrated in Scheme 1-4.

Compounds **9a-e** were generated according to Scheme 1 by following reported procedure [18]. Alkylation of commercially available 4-fluoro-3-(trifluoromethyl)benzoic acid **5** and 2-fluoroethan-1-ol generated the intermediate 4-(2-fluoroethoxy)-3-(trifluoromethyl)benzoic acid **6** under the condition of sodium hydride in dimethyl sulfoxide (DMSO). Meanwhile, the 4-position substituted amidoximes **8a-e** were prepared from corresponding benzonitriles **7a-e** reacting with hydroxylamine hydrochloride and triethylamine. Coupling of **6** with **8a-e** under the conventional peptide coupling conditions and subsequently thermally cyclization yielded the oxadiazoles **9a-e**.
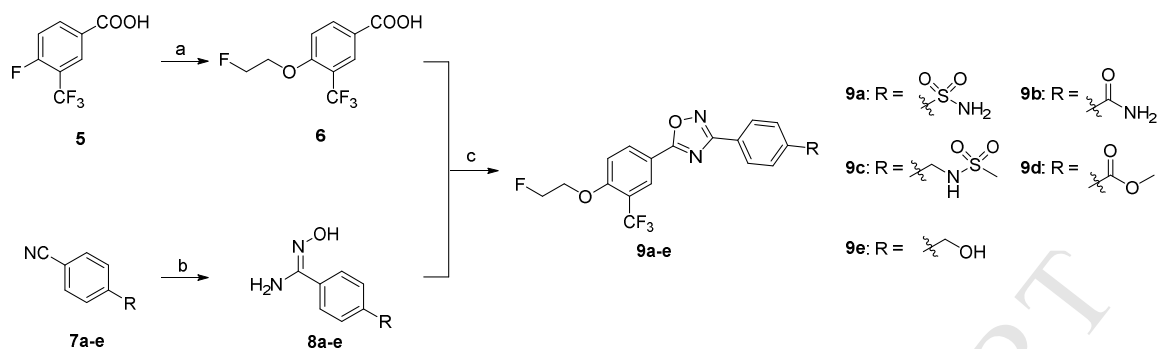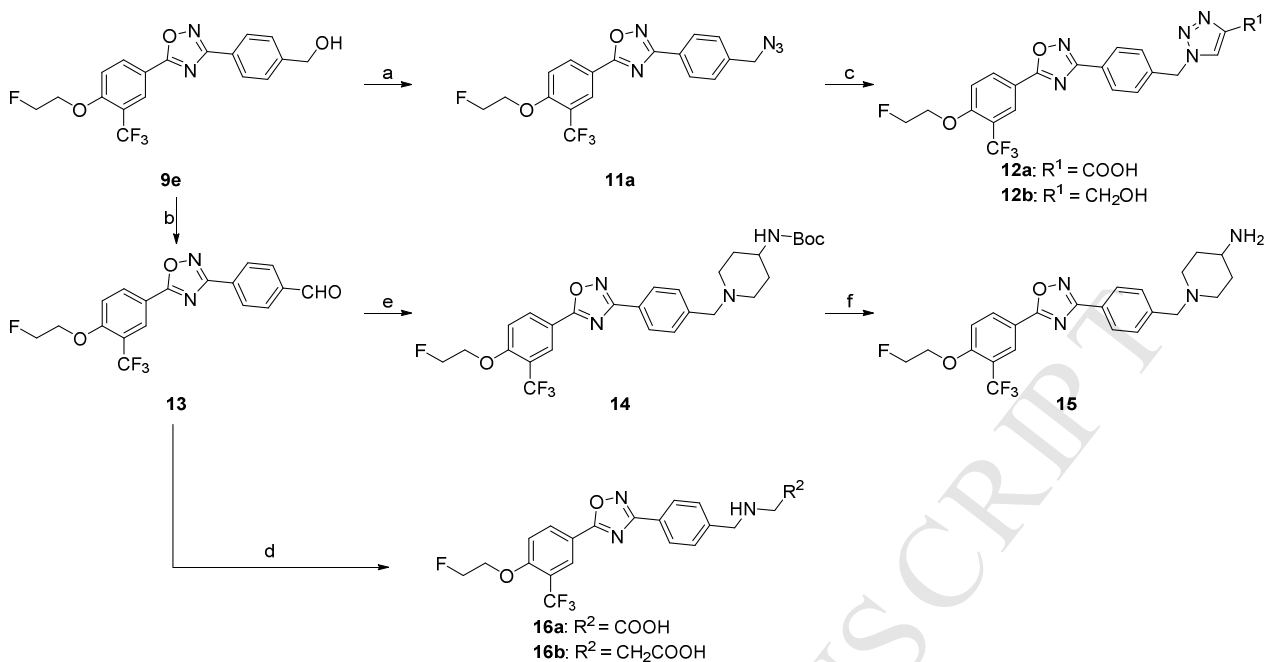
Scheme 1. Syntheses of **9a-e**. Reagents and conditions: (a) NaH, 2-fluoroethan-1-ol, DMSO, 1 M HCl, RT; (b) hydroxylamine hydrochloride, NaHCO$_3$, methanol, reflux; (c) TBTU, HOBt, DIPEA, DMF, RT-120 °C.

The syntheses of compounds **10a-c** were depicted in Scheme 2. Starting from compound **9d**, compounds **10a-c** were synthesized by the following procedures. The hydrolysis of **9d** using lithium hydroxide as base gave compound **10a**, and the ammonolysis of **9d** with hydroxylamine or hydrazine provided **10b** or **10c**, respectively.
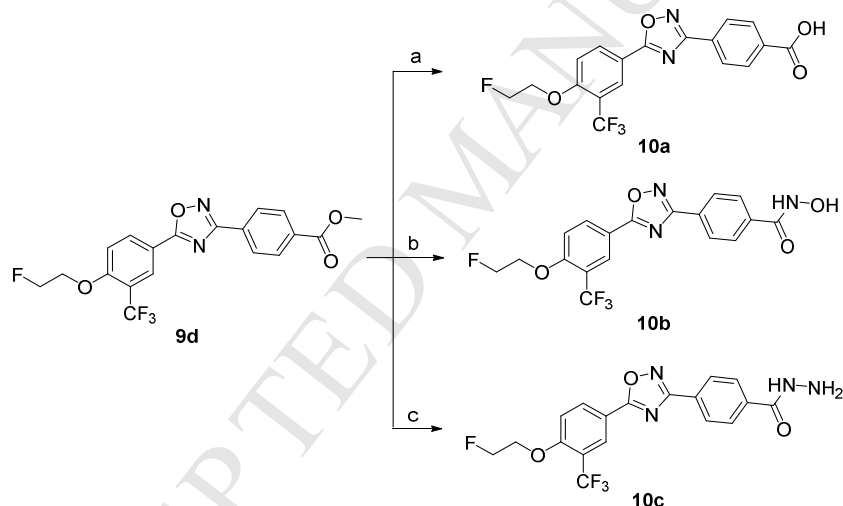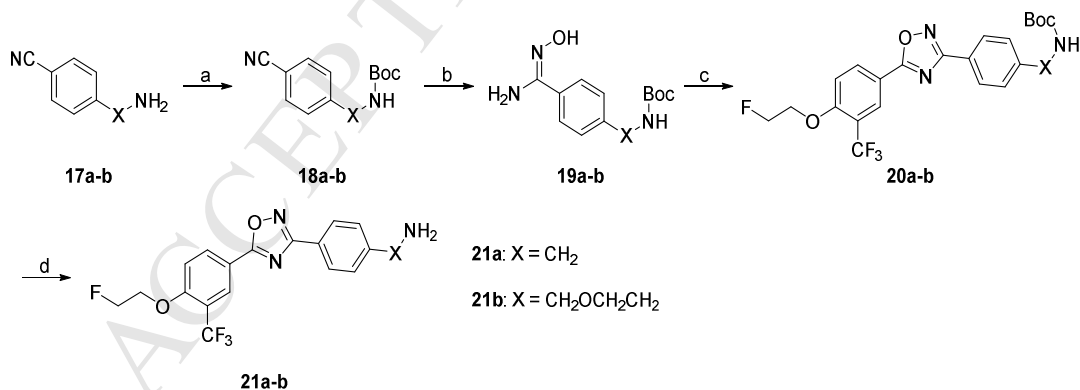

Scheme 2. Syntheses of **10a-c**. Reagents and conditions: (a) LiOH, THF, H$_2$O, RT; (b) hydroxylamine, KOH, methanol, reflux; (c) hydrazine hydrate, ethanol, reflux.

The syntheses of analogs **12a**, **12b**, **15**, and **16a-b** were illustrated in Scheme 3. The alcohol intermediate **9e** was easily transformed to azide **11a** under the condition of 1,8-diazabicyclo[5.4.0]undec-7-ene (DBU) and diphenyl phosphoryl azide (DPPA), which was used to proceed the copper(II)-catalyzed alkyne cycloaddition to afford compounds **12a-b**. The alcohol intermediate **9e** was converted to aldehyde **13** by Swern oxidation. After reductive amination from aldehyde **13** using corresponding amines afforded compounds **14** and **16a-b**. Deprotection of *tert*-butyloxycarbonyl (Boc) group of **14** using 4 M HCl in dioxane afforded compound **15**.

Scheme 3. Syntheses of **12a-b**, **15**, and **16a-b**. Reagents and conditions: (a) DPPA, DBU, toluene, 0 °C-RT; (b) oxalyl chloride, DMSO, CH$_2$Cl$_2$, triethylamine, -78 °C-RT; (c) propiolic acid or propargyl alcohol, CuSO$_4$•5H$_2$O, sodium ascorbate, THF, H$_2$O, RT; (d) NaBH$_3$CN, amines, acetic acid, methanol, RT; (e) 4-(*N*-Boc-amino)piperidine, NaBH(OAc)$_3$, acetic acid, 1,2-dichloroethane , RT; (f) 4 M HCl in dioxane, RT.

The syntheses of the analogs **21a-b** were shown in Scheme 4. Amines **17a-b** were protected using Boc group to afford **18a-b**. Oxadiazoles **20a-b** were prepared via a similar procedure shown in Scheme 1, followed by deprotection of Boc group yielded compounds **21a-b**.

Scheme 4. Syntheses of **21a-b**. Reagents and conditions: (a) di-*tert*-butyl dicarbonate, triethylamine, CH$_2$Cl$_2$, RT; (b) hydroxylamine hydrochloride, NaHCO$_3$, methanol, reflux; (c) TBTU, HOBt, DIPEA, **6**, DMF, RT-120 °C; (d) 4 M HCl in dioxane, RT.
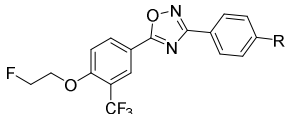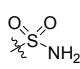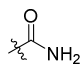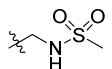
2.2. In vitro binding assay
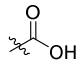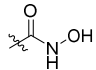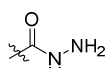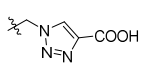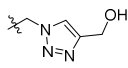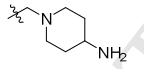
Newly synthesized compounds were firstly evaluated for binding potency toward S1PR1 by a [^{32}P]S1P competitive binding assay following published procedure [20], S1P was used as a reference compound. The

binding potency was expressed as the IC_{50} value. As shown in Table 1, most of the new analogs have good binding potency for S1PR1 with the IC_{50} values from 6.3 nM to 341 nM except compound **10a** (> 1000 nM) that has a carboxyl group. Compounds **9a** and **9c**, bearing sulfonamides group exhibited good binding potency with the IC_{50} values of 13.2 and 40.0 nM, respectively. Compound **9b**, having an amide group on the benzene ring showed a reduced potency with an IC_{50} value of 67.1 nM compared to sulfonamide compounds **9a** and **9c**. Introducing *N*-hydroxy amide or hydrazide group on the benzene ring displayed a different impact on S1PR1 binding potency. Compared to benzamide compound **9b**, benzohydrazide compound **10c** showed a 5-fold decreased IC_{50} value of 14.7 nM, but *N*-hydroxybenzamide compound **10b** exhibited a 4-fold increased IC_{50} value of 272 nM. Replacing the azetidine carboxylic acid with 1,2,3-triazole-4-carboxylic acid, 2-amino acetic acid, and 3-amino propanoic acid resulted in different S1PR1 binding potency. Compared to the IC_{50} value of compound **4** (2.6 nM [18]), 1,2,3-triazole-4-carboxylic acid containing compound **12a** (341 nM) has 130-fold increased IC_{50} value; the 2-amino acetic acid containing compound **16a** (99.8 nM) has 38-fold increased IC_{50} value; 3-amino propanoic acid containing compound **16b** (6.3 nM) has comparable binding potency. Compound **12b** showed a 35-fold decreased IC_{50} value of 9.7 nM compared to the corresponding acid **12a** (341 nM), which is also comparable to compound **4**. Replacing the azetidine carboxylic acid of compound **4** with different amines were evaluated, and the piperidine-4-amine caused the most increased IC_{50} value, the IC_{50} value of compound **15** was 156 nM; both methylamine and *O*-ethylamine caused increased IC_{50} values too (34.2 nM for **21a**, 44.2 nM for **21b**), but less increase than compound **15**. 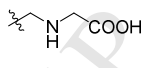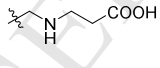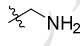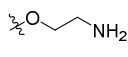The representative competitive binding curves of compounds **12b**, **16b**, and S1P for S1PR1 were displayed in Fig. 2. Our *in vitro* binding data showed that compounds **9a**, **10c**, **12b**, and **16b** were potent for S1PR1 with the IC_{50} values less than 20 nM. Consequentially, their IC_{50} values of binding to other S1P receptor subtypes S1PR2, S1PR3, S1PR4, and S1PR5 were determined to check the binding selectivity. The IC_{50} values of these four compounds binding toward S1PR1-5 were displayed in table 2. Our data showed the IC_{50} values of compounds binding toward S1PR2-5 are > 1000 nM, indicating all four compounds **9a**, **10c**, **12b**, and **16b** are selective for S1PR1 over S1PR2-5. The physicochemical properties of compounds play crucial role in brain penetration, and studies showed marketed CNS drugs were found to generally have smaller molecular weight (MW), higher calculated partition coefficient

Table 1.

Structures and binding affinities (mean ± SD) of S1P and new compounds toward S1PR1[a,b].

Compd.	R	S1PR1 IC$_{50}$ (nM)	MW	ClogP	TPSA	HBD
S1P		1.4 ± 0.3	379.5	4.1	113.0	4
9a		13.2 ± 3.2	431.4	3.4	103.3	1
9b		67.1 ± 12.6	395.3	3.7	86.3	1
9c		40.0 ± 17.8	459.4	3.7	89.4	1
10a		> 1000	396.3	4.9	80.5	1
10b		272 ± 65	411.3	3.3	92.5	2
10c		14.7 ± 1.7	410.3	3.3	98.3	2
12a		341 ± 126	477.4	4.2	108.4	1
12b		9.7 ± 1.6	463.4	3.1	91.4	1
15		156 ± 47	464.5	4.1	72.4	1
16a		99.8 ± 12.2	439.4	1.3	92.5	2
16b		6.3 ± 1.3	453.4	2.0	92.5	2
21a		34.2 ± 7.1	381.3	4.0	69.2	1
21b		44.2 ± 6.8	425.4	4.1	78.4	1

[a] IC$_{50}$ values were determined at least 3 independent experiments, each run was performed in duplicate; Assays for compounds which showed no activity (IC$_{50}$ > 1000 nM) were only repeated twice; [b] MW, ClogP, TPSA, and HBD were calculated by ChemDraw Professional 16.0.1.4 (77) (PerkinElmer Informatics, Inc.).

8
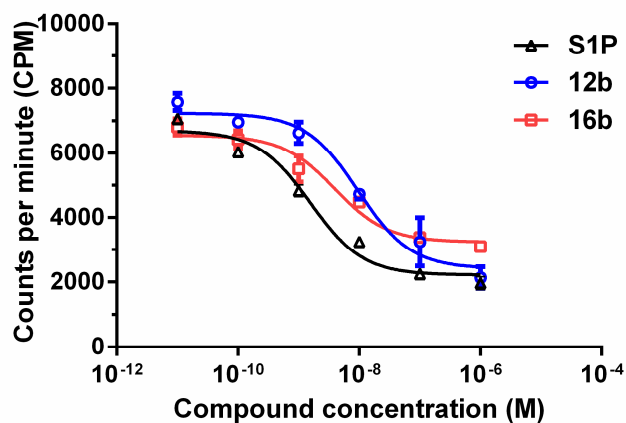
Fig. 2. The presentative competitive binding curves of compounds **12b**, **16b**, and S1P for S1PR1. A CHO cell membrane containing recombinant human S1PR1 was used in a [^{32}P]S1P competitive binding assay to measure the binding affinities. S1P (fitted $IC_{50} = 1.4 \pm 0.3$ nM) **12b** (fitted $IC_{50} = 9.7 \pm 1.6$ nM); and **16b** (fitted $IC_{50} = 6.3 \pm 1.3$ nM).

Table 2

The IC_{50} values (mean $\pm$ SD) of **S1P**, **9a**, **10c**, **12b**, and **16b** toward other S1PRs[a]

Compd.	IC_{50} (nM)				
	S1PR1	**S1PR2**	**S1PR3**	**S1PR4**	**S1PR5**
S1P	1.4 ± 0.3	3.6 ± 0.5	0.4 ± 0.2	151 ± 82	3.1 ± 1.1
9a	13.2 ± 3.2	> 1000	> 1000	> 1000	> 1000
10c	14.7 ± 1.7	> 1000	> 1000	> 1000	> 1000
12b	9.7 ± 1.6	> 1000	> 1000	> 1000	> 1000
16b	6.3 ± 1.3	> 1000	> 1000	> 1000	> 1000

[a]IC_{50} values were determined at least 3 independent experiments, each run was performed in duplicate; Assays for compounds which showed no activity ($IC_{50} > 1000$ nM) were only repeated twice.

9

(ClogP), fewer hydrogen bond donors (HBDs), and lower topological polar surface area (TPSA) compared with non-CNS drugs [21-23]. A useful guideline was concluded as follows to assess the molecules for CNS drugs: MW ≤ 470; 1 < ClogP ≤ 3; 40 < TPSA ≤ 90; and HBD ≤ 2 [24, 25]. Among these four compounds, both compounds **12b** and **16b** have good MW (463.4 and 453.4, respectively), ClogP (3.1 and 2.0, respectively), TPSA (91.4 and 92.5, respectively), and HBD (1 and 2, respectively) parameters for CNS drugs, suggesting the F-18 labeled version counterparts may have the capability of penetrating the BBB and entering the brain. Therefore, we further radiosynthesized [^{18}F]**12b** and conducted preliminary *in vivo* and *in vitro* evaluation in rats via autoradiography and *ex vivo* biodistribution study.

2.3. Radiosynthesis of [^{18}F]12b

Compound **25**, the precursor for radiolabeling [^{18}F]**12b**, was prepared by following Scheme 5. The cyclization of compound **8e** with 4-hydroxy-3-(trifluoromethyl)benzoic acid yielded compound **22**, which was converted to azide **23** in the presence of DPPA and DBU. After alkylating with ethylene ditosylate, followed by azide-alkyne cycloaddition, tosylate precursor **25** was obtained. Radiosynthesis of [^{18}F]**12b** was achieved by using the nucleophilic reaction between the tosylate precursor **25** and [^{18}F]KF in acetonitrile with Kryptofix 222 followed by deprotection of methoxymethyl (MOM) group. After purification using semi-preparative high-performance liquid chromatography (HPLC) combined with solid-phase extraction (SPE), [^{18}F]**12b** was formulated using 10% ethanol in 0.9% saline with high chemical and radiochemical purity (> 98%), good radiochemical yields (14.1 ± 2.9%), and high specific activity (54.1 ± 8.3 GBq/μmol, n = 6, decay corrected to EOS). The representative radio-UV analytical HPLC chromatograms (Fig. S1) and method were presented in the supporting material. It took approximately 90 min for the total radiosynthesis.
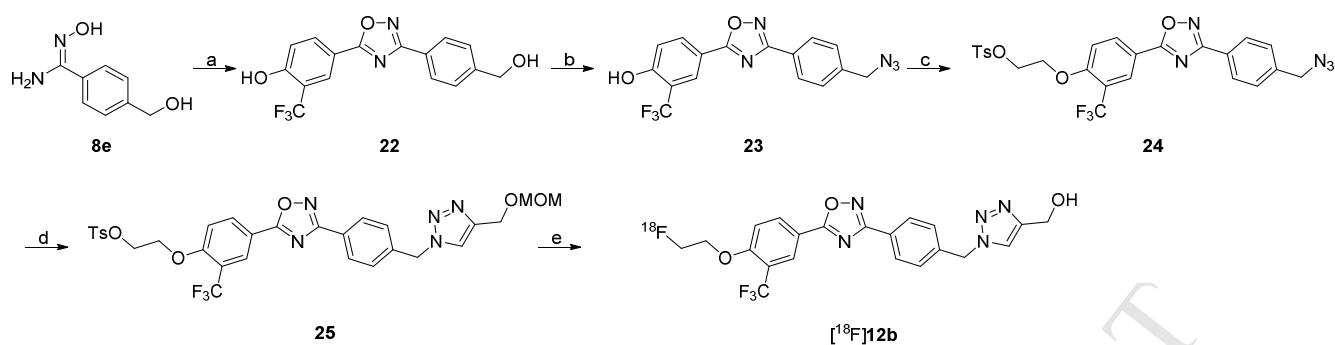
Scheme 5 Syntheses of the precursor **25** and [^{18}F]**12b**. Reagents and conditions: (a) 4-hydroxy-3-(trifluoromethyl)benzoic acid, TBTU, HOBt, DIPEA, DMF, RT-120 °C; (b) DPPA, DBU, toluene, 0 °C, RT; (c) ethylene ditosylate, K_2CO_3, CH_3CN, 90 °C; (d) 3-(methoxymethyl)prop-1-yne, $CuSO_4 \cdot 5H_2O$, sodium ascorbate, THF, H_2O, RT; (e) [^{18}F]KF, Kryptofix 222, K_2CO_3, CH_3CN, 110 °C, 15 min, 6 M HCl, 110 °C, 5 min, 6 M NaOH.

2.4. *Ex vivo autoradiography study of [^{18}F]12b in normal rat*

Ex vivo autoradiography study was performed to check if [^{18}F]**12b** is able to cross the BBB in the rat. An adult male Sprague-Dawley (SD) rat was tail intravenously (i.v.) injected with [^{18}F]**12b** and euthanized at 60 min post-injection. The brain was immediately removed and snap-frozen followed by sectioning and mounting on glass slides. The brain sections were exposed and the distribution of radioactivity was visualized by a Bio-Imaging analyzer. As shown in Fig. 3, [^{18}F]**12b** was able to cross the BBB and showed high uptake in the rat brain, which is consistent to the expression of S1PR1 in the brain of rodents and human [26-28].
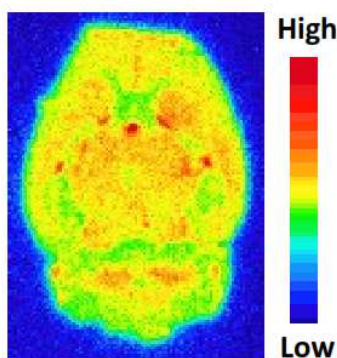

Fig. 3. *Ex vivo* autoradiography of [^{18}F]**12b** in rat brain.

2.5. *In vitro autoradiography study of [^{18}F]12b in LPS-treated mice*

To confirm the binding specificity of [^{18}F]**12b** toward S1PR1, *in vitro* autoradiography studies were performed using mouse brain slices that generated from LPS-induced murine neuroinflammation model, a

widely used model for neuroinflammation, and the expression of S1PR1 was activated in the mouse brain following the LPS injection according to the report [29]. SEW2871, an S1PR1-specific ligand (IC_{50} = 37 nM) [30] was used as a blocking agent. Adult male C57BL/6 mice were euthanized at 24 h after receiving an intraperitoneal injection of LPS, brain tissues were collected and sectioned. For the control study, the slices were incubated with [^{18}F]**12b**; for the blocking study, slices were incubated with [^{18}F]**12b** in the presence of SEW2871 at 10 μM of concentration. *In vitro* autoradiography study showed that SEW2871 was able to reduce the uptake of [^{18}F]**12b** by ~36%, suggesting the binding of [^{18}F]**12b** toward S1PR1 is specific (Fig. 4).
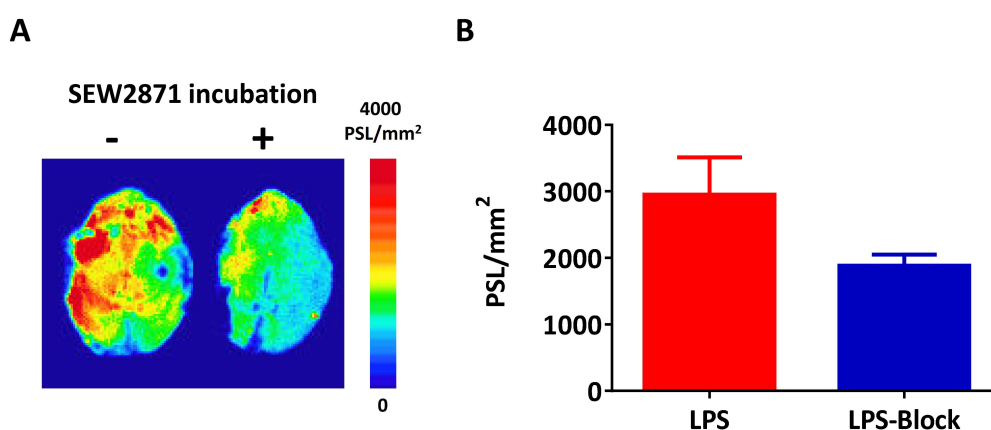
Fig. 4. Representative *in vitro* autoradiographic images (A) and quantification of autoradiography (B) of brain sections from LPS-induced neuroinflammation mice under control or blocking condition. SEW2871, an S1PR1-specific ligand (IC_{50} = 37 nM), was used as the blocking agent.

2.6. Biodistribution study of [^{18}F]**12b** in rats

To further investigate the tissue distribution of [^{18}F]**12b** in rodents, the *ex vivo* biodistribution study was performed in adult female Lewis rats. Animals were euthanized at 5, 30, 60, and 120 min post-injection. As shown in the Table 3, the initial uptake (ID%/g) at 5 min post injection in blood, heart, lung, muscle, fat, pancreas, spleen, kidney, liver, bone, thymus, and brain was 0.49, 1.65, 2.79, 0.39, 0.51, 1.96, 2.22, 3.43, 5.69, 0.55, 0.69, and 0.49, respectively. A rapid clearance of radioactivity was observed in tissues heart, lung, spleen, kidney, and liver; uptake (ID%/g) was decreased to 1.19, 1.96, 1.36, 2.11, and 4.30 at 30 min from 1.65, 2.79, 2.22, 3.43, and 5.69 at 5 min, respectively. The radioactivity accumulation in the bone has no change from 5 min to 120 min, suggesting [^{13}F]**12b** had no defluorination *in vivo*. A high uptake (ID%/g) of [^{18}F]**12b** in the

brain was observed compared to radiotracer [^{18}F]**4** [18]. The brain uptake (ID%/g) of [^{18}F]**12b** was 0.49, 0.57, 0.71, and 0.61 at 5, 30, 60, and 120 min, respectively. In brain regions including cerebellum, brain stem, cortex, striatum, thalamus, and hippocampus, [^{18}F]**12b** had similar distribution, the uptake (ID%/g) in each region was 0.53, 0.50, 0.59, 0.47, 0.46, and 0.43, respectively at 5 min; the brain uptake at 60 min post injection reached the maximum, then gradually washed out as shown in Fig. 5. Our data suggested that [^{18}F]**12b** has the potential to be a PET tracer for imaging S1PR1 expression in the brain *in vivo*.

Table 3.

Biodistribution of [^{18}F]**12b** in female Lewis rats.(%ID/g values, mean ± SD, n = 4).

Organs	Tissue uptake (%ID/g)			
	5 min	30 min	60 min	120 min
Blood	0.49 ± 0.07	0.42 ± 0.05	0.36 ± 0.02	0.35 ± 0.01
Heart	1.65 ± 0.27	1.19 ± 0.06	1.05 ± 0.08	0.94 ± 0.06
Lung	2.79 ± 0.57	1.96 ± 0.07	1.67 ± 0.09	1.54 ± 0.07
Muscle	0.39 ± 0.04	0.59 ± 0.05	0.51 ± 0.02	0.47 ± 0.02
Fat	0.51 ± 0.22	0.62 ± 0.10	0.69 ± 0.07	0.57 ± 0.07
Pancreas	1.96 ± 0.56	1.89 ± 0.16	1.52 ± 0.25	1.45 ± 0.15
Spleen	2.22 ± 0.23	1.36 ± 0.04	1.27 ± 0.08	1.14 ± 0.10
Kidney	3.43 ± 0.31	2.11 ± 0.08	1.91 ± 0.10	1.62 ± 0.09
Liver	5.69 ± 0.60	4.30 ± 0.37	4.21 ± 0.21	3.66 ± 0.14
Bone	0.55 ± 0.05	0.45 ± 0.03	0.45 ± 0.01	0.51 ± 0.05
Thymus	0.69 ± 0.08	0.83 ± 0.07	0.82 ± 0.04	0.78 ± 0.05
Brain	0.49 ± 0.04	0.57 ± 0.02	0.71 ± 0.03	0.61 ± 0.05
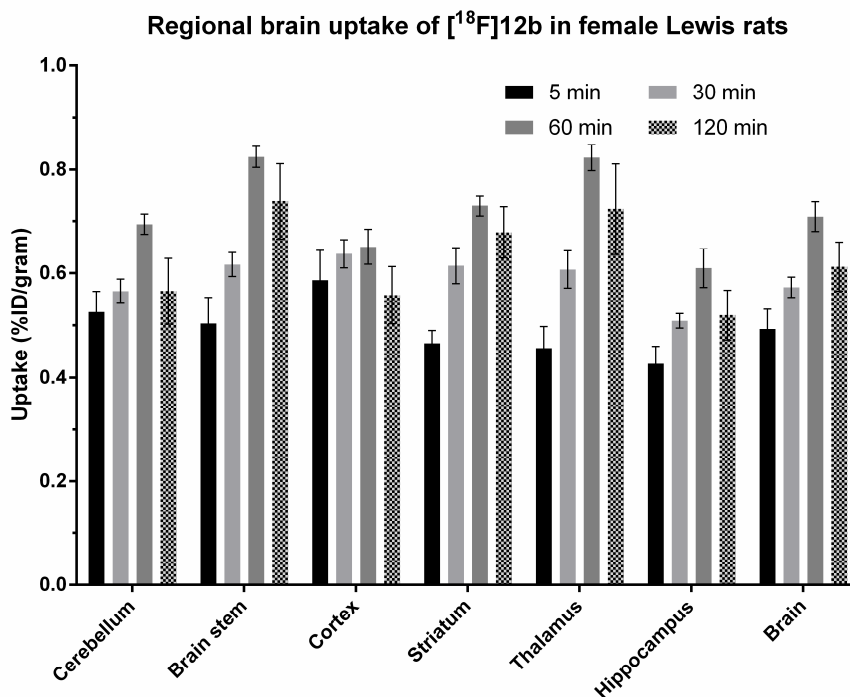
Fig. 5. Regional brain uptake of [^{18}F]**12b** in female Lewis rats. Animals were sacrificed at 5, 30, 60, and 120 min post-injection. %ID/gram values (mean ± SD) with 4 rats per group.

3. Conclusion

In summary, we explored the structure of lead compound **4** to afford new S1PR1 compounds by replacing the 3-*N*-azetedinyl carboxyl acid with different hydrophilic groups. Thirteen new analogs were synthesized and their *in vitro* binding affinities were determined. Four compounds **9a**, **10c**, **12b**, and **16b** had high S1PR1 binding potency with IC$_{50}$ values ranging from 6.3 to 15 nM and also displayed highly selective for S1PR1 versus other S1P receptor subtypes (IC$_{50}$ > 1000 nM for S1PR2-5). Radiosynthesis of [^{18}F]**12b** was accomplished with good yield and high purity. Our initial evaluation of [^{18}F]**12b** in rodent using autoradiography and biodistribution studies indicated [^{18}F]**12b** was able to penetrate the BBB and had good brain retention; no defluorination was observed *in vivo*. *In vitro* autoradiography study in brain slices of LPS-induced neuroinflammation mice indicated that SEW2871, a specific S1PR1 ligand was able to reduce the uptake of [^{18}F]**12b**, suggesting that [^{18}F]**12b** had specific binding toward S1PR1. Further *in vivo* evaluation of

14

[^{18}F]**12b** in animal models of neuroinflammatory diseases warrants the suitability of [^{18}F]**12b** to be an S1PR1 specific PET radiotracer for assessing inflammation response in CNS.

4. Experimental section

4.1. General

Commercially available starting materials, reagents, and solvents were used as purchased without further purification unless otherwise stated. Reactions were monitored by thin-layer chromatography (TLC) carried out on pre-coated glass plates of silica gel 60 F$_{254}$ from EMD Chemicals Inc. Visualization was accomplished with ultraviolet light (UV 254 nm). Compounds were purified by recrystallization or flash column chromatography using 230–400 mesh silica gel purchased from Silicycle. Melting points were determined on a MEL-TEMP 3.0 apparatus without corrected. ^{1}H NMR and ^{13}C NMR spectra were received from Varian 400 MHz instrument. Chemical shifts were reported in parts per million (ppm) and were calibrated using a residual undeuterated solvent as an internal reference (CDCl$_3$: δ 7.26 ppm; CD$_3$OD: δ 3.31 ppm; DMSO-*d6*: δ 2.50 ppm; Acetone-*d6*: δ 2.05 ppm). High-resolution positive ion mass was acquired by a Bruker MaXis 4G Q-TOF mass spectrometer with electrospray ionization source.

All animal experiments were conducted under Washington University's Institutional Animal Care and Use Committee (IACUC)-approved protocols in accordance with the US National Research Council's Guide for the Care and Use of Laboratory Animals.

4.2. Chemistry

4.2.1. Synthesis of **9a-e**

4-(2-Fluoroethoxy)-3-(trifluoromethyl)benzoic acid (6). To a round-bottom flask equipped with a stir bar was added 4-fluoro-3-(trifluoromethyl)benzoic acid (8.32 g, 40.0 mmol), 2-fluoroethanol (3.84 g, 60 mmol), and DMSO (100 mL) under N$_2$ atmosphere. NaH (2.07 g, 90.0 mmol) was added portion wise with stirring. The reaction was stirred at room temperature overnight and monitored by TLC. The mixture was poured into ice-

water (1 L) and acidified with 1 M HCl to give a precipitate. The resulting precipitate was filtered off, washed with water and hexanes to give a tan solid (9.6 g, 95%). MP: 131-133 °C. ^{1}H NMR (400 MHz, DMSO-*d6*) δ 13.18 (br, 1H, *-COOH*), 8.37 – 8.04 (m, 2H, *-ArH*), 7.45 – 7.32 (m, 1H, *-ArH*), 4.89 – 4.74 (m, 1H, *-CH$_2$F*), 4.72 – 4.58 (m, 1H, *-CH$_2$F*), 4.52 – 4.39 (m, 1H, *-CH$_2$O-*), 4.38 – 4.29 (m, 1H, *-CH$_2$O-*).

General procedure for the synthesis of 8a-e. To a round-bottom flask equipped with a stir bar was added **7a-e** (1.0 eq), hydroxylamine hydrochloride (2.0 eq), NaHCO$_3$ (4.0 eq), and methanol (5.0 mL/mmol). The reaction was refluxed and stirred in a pre-heated 75 °C oil-bath for 6 h. The reaction mixture was cooled to room temperature, and the precipitate was filtered off and washed with methanol. The filtrate was concentrated *in vacuo* without further purification.

(*E*)-*N*′-hydroxy-4-sulfamoylbenzimidamide (8a). Yield: 70%. MP: 217-219 °C. ^{1}H NMR (400 MHz, DMSO-*d6*) δ = 7.88-7.78 (m, 4H, *-ArH*), 5.93 (s, 2H, *-SO$_2$NH$_2$*).

(*E*)-4-(*N*′-hydroxycarbamimidoyl)benzamide (8b). Yield: 39%. MP: 221-224 °C. ^{1}H NMR (400 MHz, DMSO-*d6*) δ 9.78 (s, 1H, *-OH*), 7.98 (s, 1H,*-NH$_2$*), 7.86 (d, *J* = 8.4 Hz, 2H, *-ArH*), 7.74 (d, *J* = 8.4 Hz, 2H, *-ArH*), 7.38 (s, 1H, *-NH$_2$*), 5.88 (s, 2H, *-CONH$_2$*).

(*E*)-*N*′-hydroxy-4-(methylsulfonamidomethyl)benzimidamide (8c). Yield: 95%. MP: 178-180 °C. ^{1}H NMR (300 MHz, DMSO-*d6*) δ 9.62 (s, 1H, *-OH*), 7.63 (d, *J* = 8.3 Hz, 2H, *-ArH*), 7.32 (d, *J* = 8.4 Hz, 2H, *-ArH*), 5.78 (s, 2H, *-NH$_2$*), 4.14 (s, 2H, *-CH$_2$-*), 2.84 (s, 3H, *-CH$_3$*).

Methyl (*E*)-4-(*N*′-hydroxycarbamimidoyl)benzoate (8d). Yield: 86%. MP: 168-170 °C. ^{1}H NMR (400 MHz, DMSO-*d6*) δ = 9.91 (s, 1H, *-OH*), 7.94 (d, *J* = 8.0 Hz, 2H, *-ArH*), 7.82 (d, *J* = 8.4 Hz, 2H, *-ArH*), 5.93 (s, 2H, *-NH$_2$*), 3.85 (s, 3H, *-OCH$_3$*)

(*E*)-*N*′-hydroxy-4-(hydroxymethyl)benzimidamide (8e). Yield: 76%. MP: 152-155 °C. ^{1}H NMR (400 MHz, DMSO-*d6*) δ 9.57 (s, 1H, *-OH*), 7.71 – 7.57 (m, 2H, *-ArH*), 7.37 – 7.24 (m, 2H, *-ArH*), 5.77 (s, 2H, *-NH$_2$*), 5.24 (s, 1H, *-CH$_2$OH*), 4.51 (s, 2H, *-CH$_2$-*).

General procedure for the synthesis of 9a-e. To a round-bottom flask equipped with a stir bar was added acid **6** (1.0 eq), HOBt (0.2 eq), TBTU (1.0 eq), DIPEA (3.0 eq), and DMF (5.0 mL/mmol). The reaction mixture was stirred for 0.5 h followed by adding amidoxime **8a-e** (1.0 eq). The reaction mixture was stirred for 1 h at room

16

temperature, then refluxed in a pre-heated 120 °C oil-bath for 4 h and monitored by TLC. After cooling, the reaction mixture was diluted with water and extracted with ethyl acetate. The ethyl acetate layer was washed with 1 M HCl, saturated brine, and dried over anhydrous $MgSO_4$. After filtration and concentration, the residue was purified on a silica gel column.

4-(5-(4-(2-Fluoroethoxy)-3-(trifluoromethyl)phenyl)-1,2,4-oxadiazol-3-yl)benzenesulfonamide (9a). Yield: 51%. MP: 198-199 °C. ^{1}H NMR (400 MHz, DMSO-*d6*) δ 8.45 – 8.38 (m, 1H, *-ArH*), 8.33 – 8.24 (m, 3H, *-ArH*), 8.04 (d, *J* = 8.4 Hz, 2H, *-ArH*), 7.62 – 7.52 (m, 3H, *-ArH&-NH₂*), 4.89 – 4.81 (m, 1H, *-CH₂F*), 4.76 – 4.70 (m, 1H, *-CH₂F*), 4.61 – 4.55 (m, 1H, *-CH₂O-*), 4.54 – 4.44 (m, 1H, *-CH₂O-*). ^{13}C NMR (101 MHz, DMSO-*d6*) δ 174.92, 167.79, 160.02, 147.12, 134.58, 129.34, 128.21, 127.08 (q, *J* = 5.1 Hz), 127.04, 123.31 (d, *J* = 272.7 Hz), 118.61 (q, *J* = 31.3 Hz), 116.10, 115.44, 82.10 (d, *J* = 168.7 Hz), 69.24 (d, *J* = 18.2 Hz). HRMS (ESI) calcd for $C_{17}H_{13}F_4N_3O_4S$ [M + H⁺] 432.0636. Found [M + H⁺] 432.0640.

4-(5-(4-(2-Fluoroethoxy)-3-(trifluoromethyl)phenyl)-1,2,4-oxadiazol-3-yl)benzamide (9b). Yield: 29%. MP: 244-245 °C. ^{1}H NMR (400 MHz, DMSO-*d6*) δ 8.40 (d, *J* = 8.1 Hz, 1H, *-ArH*), 8.30 (s, 1H, *-ArH*), 8.19 – 8.10 (m, 3H, *-ArH&-NH₂*), 8.10 – 8.03 (m, 2H, *-ArH*), 7.59 – 7.51 (m, 2H, *-ArH*), 4.89 – 4.82 (m, 1H, *-CH₂F*), 4.76 – 4.71 (m, 1H, *-CH₂F*), 4.62 – 4.55 (m, 1H, *-CH₂O-*), 4.53 – 4.47 (m, 1H, *-CH₂O-*). ^{13}C NMR (101 MHz, DMSO-*d6*) δ 174.72, 168.14, 167.49, 159.96, 137.42, 134.54, 128.77, 127.42, 127.08 (q, *J* = 5.1 Hz), 123.31 (d, *J* = 273.7 Hz), 118.58 (q, *J* = 31.3 Hz), 116.17, 115.41, 82.10 (d, *J* = 168.7 Hz), 69.23 (d, *J* = 19.2 Hz). HRMS (ESI) calcd for $C_{18}H_{13}F_4N_3O_3$ [M + H⁺] 396. 0966. Found [M + H⁺] 396.0959.

***N*-(4-(5-(4-(2-Fluoroethoxy)-3-(trifluoromethyl)phenyl)-1,2,4-oxadiazol-3-yl)benzyl)methanesulfonamide (9c)**. Yield: 9%. MP: 208-300 °C. ^{1}H NMR (400 MHz, DMSO-*d6*) δ 8.41 (d, *J* = 8.9 Hz, 1H, *-ArH*), 8.31 (s, 1H, *-ArH*), 8.07 (d, *J* = 8.1 Hz, 2H, *-ArH*), 7.73 – 7.67 (m, 1H, *-ArH*), 7.61 – 7.52 (m, 3H, *-ArH&-NHSO₂-*), 4.89 – 4.81 (m, 1H, *-CH₂F*), 4.78 – 4.70 (m, 1H, *-CH₂F*), 4.63 – 4.56 (m, 1H, *-CH₂O-*), 4.55 – 4.48 (m, 1H, *-CH₂O-*), 4.26 (d, *J* = 6.3 Hz, 2H, *-ArCH₂-*), 2.91 (s, 3H, *-SO₂CH₃*). ^{13}C NMR (101 MHz, DMSO-*d6*) δ 174.54, 168.46, 159.91, 142.71, 134.54, 128.77, 127.64, 127.07 (q, *J* = 5.1 Hz), 125.29, 123.34 (d, *J* = 273.7 Hz), 118.56 (q, *J* = 31.3 Hz), 116.31, 115.43, 82.12 (d, *J* = 168.7 Hz), 69.23 (d, *J* = 18.2 Hz), 46.13, 40.35. HRMS (ESI) calcd for $C_{19}H_{17}F_4N_3O_4S$ [M + H⁺] 460.0949. Found [M + H⁺] 460.0936.

17

Methyl 4-(5-(4-(2-fluoroethoxy)-3-(trifluoromethyl)phenyl)-1,2,4-oxadiazol-3-yl)benzoate (9d). Yield: 62%. MP: 166-169 °C. ^{1}H NMR (400 MHz, Acetone-*d6*) δ 8.45 (d, *J* = 8.9 Hz, 1H, *-ArH*), 8.42 (s, 1H, *-ArH*), 8.26 (d, *J* = 8.1 Hz, 2H, *-ArH*), 8.18 (d, *J* = 8.2 Hz, 2H, *-ArH*), 7.57 (d, *J* = 8.7 Hz, 1H, *-ArH*), 4.96 – 4.92 (m, 1H, *-CH$_2$F*), 4.85 – 4.80 (m, 1H, *-CH$_2$F*), 4.68 – 4.64 (m, 1H, *-CH$_2$O-*), 4.62 – 4.56 (m, 1H, *-CH$_2$O-*), 3.94 (s, 3H, *-OCH$_3$*). ^{13}C NMR (101 MHz, Acetone-*d6*) δ 174.80, 168.03, 165.62, 160.06, 133.86, 132.69, 130.76, 129.94, 127.34, 126.97 (q, *J* = 5.1 Hz), 123.12 (d, *J* = 273.7 Hz), 119.22 (d, *J* = 31.3 Hz), 116.41, 114.50, 81.54 (d, *J* = 169.7 Hz), 68.95 (d, *J* = 19.2 Hz), 51.75.

(4-(5-(4-(2-Fluoroethoxy)-3-(trifluoromethyl)phenyl)-1,2,4-oxadiazol-3-yl)phenyl)methanol (9e) [18]. Yield: 65%. MP: 190-192 °C. ^{1}H NMR (400 MHz, CDCl$_3$) δ = 8.45 (d, *J* = 2.0 Hz, 1H, *-ArH*), 8.33 (dd, *J* = 8.8 Hz, 2.0 Hz, 1H, *-ArH*), 8.13 (d, *J* = 8.0 Hz, 2H, *-ArH*), 7.50 (d, *J* = 8.0 Hz, 2H, *-ArH*), 7.16 (d, *J* = 8.4 Hz, 1H, *-ArH*), 4.90–4.74 (m, 4H, *-CH$_2$F &-CH$_2$OH*), 4.48–4.35 (m, 2H, *-CH$_2$O-*).

*4.2.2. Synthesis of **10a-c***

4-(5-(4-(2-Fluoroethoxy)-3-(trifluoromethyl)phenyl)-1,2,4-oxadiazol-3-yl)benzoic acid (10a). To a round-bottom flask equipped with a stir bar was added ester **9d** (2.0 g, 4.87 mmol), lithium hydroxide (230 mg, 9.75 mmol), THF (20 mL), and water (4 mL). The reaction mixture was stirred overnight and acidified with 1 M HCl to pH = 1. The reaction mixture was extracted with ethyl acetate (20 mL), and the ethyl acetate layer was washed with saturated brine, and dried over anhydrous MgSO$_4$. After filtration and concentration, **10a** was obtained as an off-white solid. (1.7 g, 87%). MP: 220-222 °C. ^{1}H NMR (400 MHz, DMSO-*d6*) δ 13.26 (s, 1H, *-COOH*), 8.39 (d, *J* = 8.8 Hz, 1H, *-ArH*), 8.28 (s, 1H, *-ArH*), 8.19 – 8.08 (m, 4H, *-ArH*), 7.54 (d, *J* = 8.8 Hz, 1H, *-ArH*), 4.91 – 4.81 (m, 1H, *-CH$_2$F*), 4.79 – 4.69 (m, 1H, *-CH$_2$F*), 4.63 – 4.47 (m, 2H, *-CH$_2$O-*). ^{13}C NMR (101 MHz, DMSO-*d6*) δ 174.80, 168.02, 167.02, 159.98, 134.55, 133.84, 130.13, 129.85, 127.70, 127.07 (q, *J* = 5.1 Hz), 123.30 (d, *J* = 273.7 Hz), 118.57 (q, *J* = 31.3 Hz), 116.11, 115.41, 82.09 (d, *J* = 168.7 Hz), 69.22 (d, *J* = 19.2 Hz).

4-(5-(4-(2-Fluoroethoxy)-3-(trifluoromethyl)phenyl)-1,2,4-oxadiazol-3-yl)-*N*-hydroxybenzamide (10b). To a round-bottom flask equipped with a stir bar was added ester **9d** (150 mg, 0.37 mmol), hydroxylamine

hydrochloride (76 mg, 1.1 mmol) and methanol (1.9 mL), followed by adding potassium hydroxide (12.5 mg, 2.22 mmol). The reaction mixture was refluxed overnight. After cooling to room temperature, the mixture was diluted with water (20 mL) to precipitate the product. The precipitate was filtered off and washed with diethyl ether to give an off-white solid (111 mg, 73%). MP: 186-189 °C. ^{1}H NMR (400 MHz, DMSO-*d6*) δ 11.43 (s, 1H, *-OH*), 9.20 (s, 1H, *-NH-*), 8.42 (d, *J* = 8.1 Hz, 1H, *-ArH*), 8.31 (s, 1H, *-ArH*), 8.18 – 8.11 (m, 2H, *-ArH*), 8.01 – 7.91 (m, 2H, *-ArH*), 7.61 – 7.51 (m, 1H, *-ArH*), 4.92 – 4.68 (m, 2H, *-CH2F*), 4.64 – 4.47 (m, 2H, *-CH2O-*). ^{13}C NMR (101 MHz, DMSO-*d6*) δ 174.77, 168.12, 167.05, 159.99, 135.95, 134.59, 130.55, 128.23, 127.59, 127.12 (d, *J* = 5.1 Hz), 123.31 (d, *J* = 274.7 Hz), 118.57 (*J* = 30.3 Hz), 116.19, 115.45, 82.11 (d, *J* = 168.7 Hz), 69.24 (d, *J* = 19.2 Hz). HRMS (ESI) calcd for $C_{18}H_{13}F_4N_3O_4$ [M + H$^+$] 412.0919. Found [M + H$^+$] 412.0915.

4-(5-(4-(2-Fluoroethoxy)-3-(trifluoromethyl)phenyl)-1,2,4-oxadiazol-3-yl)benzohydrazide (10c). To a round-bottom flask equipped with a stir bar was added ester **9d** (205 mg, 0.5 mmol), ethanol (1.3 mL), and hydrazine monohydrate (0.07 mL, 1.5 mmol). The reaction mixture was refluxed overnight. After cooling to room temperature, the precipitate was filtered off and washed with diethyl ether to give an off-white solid. (100 mg, 49%). MP: 186-188 °C. ^{1}H NMR (400 MHz, DMSO-*d6*) δ 9.98 (s, 1H, *-CONH-*), 8.42 (d, *J* = 8.7 Hz, 1H, *-ArH*), 8.32 (s, 1H, *-ArH*), 8.14 (d, *J* = 8.2 Hz, 2H, *-ArH*), 8.01 (d, *J* = 8.2 Hz, 2H, *-ArH*), 7.56 (d, *J* = 8.8 Hz, 1H, *-ArH*), 4.89 – 4.81 (m, 1H, *-CH2F*), 4.77 – 4.70 (m, 1H, *-CH2F*), 4.68 – 4.55 (m, 3H, *-CH2O-&-NH2*), 4.55 – 4.48 (m, 1H, *-CH2O-*). ^{13}C NMR (101 MHz, DMSO-*d6*) δ 174.75, 168.14, 165.35, 159.98, 136.46, 134.57, 128.62, 128.30, 127.52, 127.11 (q, *J* = 5.1 Hz), 123.32 (d, *J* = 273.7 Hz), 118.60 (q, *J* = 31.3 Hz), 116.20, 115.46, 82.11 (d, *J* = 167.7 Hz), 69.25 (d, *J* = 19.2 Hz). HRMS (ESI) calcd for $C_{18}H_{14}F_4N_4O_3$ [M + H$^+$] 411.1075. Found [M + H$^+$] 411.1067.

*4.2.3. Synthesis of **12a-b**, **15**, and **16a-b***

3-(4-(Azidomethyl)phenyl)-5-(4-(2-fluoroethoxy)-3-(trifluoromethyl)phenyl)-1,2,4-oxadiazole (11a). To a round-bottom flask equipped with a stir bar was added **9e** (1.0 g, 2.62 mmol), diphenyl phosphoryl azide (0.86 g, 3.14 mmol), and toluene (5.0 mL). The mixture was cooled to 0 °C before adding 1,8-diazabicyclo[5.4.0]undec-7-ene (0.48, 3.14 mmol) dropwise. The reaction was warmed to room temperature slowly and stirred overnight.

Then, the reaction mixture was diluted with water (20 mL) and extracted with ethyl acetate (30 mL). The ethyl acetate layer was washed with 1 M HCl, saturated brine and dried over anhydrous MgSO$_4$. After filtration and concentration, the residue was purified on a silica gel column, eluted with ethyl acetate/hexanes (V/V, 3/7) to give a white solid. (330 mg, 62%). MP: 117-119 °C. ^{1}H NMR (400 MHz, CDCl$_3$) δ = 8.47 (d, J = 2.0 Hz, 1H, -*ArH*), 8.35 (dd, J = 8.8 Hz, 2.0 Hz, 1H, -*ArH*), 8.19 (d, J = 8.4 Hz, 2H, -*ArH*), 7.47 (d, J = 8.0 Hz, 2H, -*ArH*), 7.18 (d, J = 8.8 Hz, 1H, -*ArH*), 4.94 – 4.73 (m, 2H, -*CH$_2$F*), 4.50 – 4.35 (m, 4H, -*CH$_2$O-&-CH$_2$N$_3$*). ^{13}C NMR (101 MHz, Acetone-*d6*) δ 174.54, 168.40, 159.98, 139.55, 133.81, 129.35, 128.89, 127.60, 126.92 (q, J = 5.1 Hz), 123.15 (d, J = 273.7 Hz), 119.21 (d, J = 31.3 Hz), 116.60, 114.50, 81.55 (d, J = 169.7 Hz), 68.94 (d, J = 20.2 Hz), 53.69.

General procedure for the synthesis of 12a-b. To a round-bottom flask equipped with a stir bar was added azide **11a** (1.0 eq) and THF. Once the azide was dissolved, water (0.6 mL/mmol) was added followed by propiolic acid or propargyl alcohol (1.05 eq), sodium ascorbate (0.10 eq), and copper sulfate pentahydrate (0.06 eq). The reaction mixture was stirred for 4 h and monitored by TLC. Then, the reaction mixture was diluted with water and extracted with ethyl acetate. The ethyl acetate layer was washed with saturated brine and dried over anhydrous MgSO$_4$. After filtration and concentration, a yellow solid was obtained.

1-(4-(5-(4-(2-Fluoroethoxy)-3-(trifluoromethyl)phenyl)-1,2,4-oxadiazol-3-yl)benzyl)-1*H*-1,2,3-triazole-4-carbox-ylic acid (12a). MP: 157-158 °C. ^{1}H NMR (400 MHz, DMSO-*d6*) δ 13.09 (s, 1H, -*COOH*), 8.86 (s, 1H, -*ArH*), 8.41 (d, J = 8.2 Hz, 1H, -*ArH*), 8.30 (s, 1H, -*ArH*), 8.10 (d, J = 7.5 Hz, 2H, -*ArH*), 7.53 (d, J = 7.7 Hz, 2H, -*ArH*), 7.17 – 7.11 (m, 1H, -*ArH*), 5.78 (s, 2H, -*ArCH$_2$-*), 4.88 – 4.46 (m, 4H, -*OCH$_2$CH$_2$F*). ^{13}C NMR (101 MHz, DMSO-*d6*) δ 174.64, 168.26, 162.01, 159.93, 140.38, 139.55, 134.57, 129.31, 129.20, 128.04, 127.08 (d, J = 5.1 Hz), 123.32 (d, J = 274.7 Hz), 120.33, 118.56 (q, J = 31.3 Hz), 116.24, 115.43, 82.11 (d, J = 167.7 Hz), 69.23 (d, J = 19.2 Hz), 53.04. HRMS (ESI) calcd for C$_{21}$H$_{15}$F$_4$N$_5$O$_4$ [M + H$^+$] 478.1133. Found [M + H$^+$] 478.1125.

(1-(4-(5-(4-(2-Fluoroethoxy)-3-(trifluoromethyl)phenyl)-1,2,4-oxadiazol-3-yl)benzyl)-1H-1,2,3-triazol-4-yl)met-hanol (12b). MP: 175-177 °C. ^{1}H NMR (400 MHz, DMSO-*d6*) δ 8.41 (d, J = 8.6 Hz, 1H, -*ArH*), 8.30 (s, 1H, -*ArH*), 8.08 (d, J = 4.7 Hz, 3H, -*ArH*), 7.60 – 7.45 (m, 3H, -*ArH*), 5.70 (s, 2H, -*ArCH$_2$-*), 5.20 (s, 1H, -*OH*),

4.89 – 4.67 (m, 2H, -*CH₂F*), 4.63 – 4.48 (m, 4H, -*CH₂O- & -CH₂OH*). ^{13}C NMR (101 MHz, DMSO-*d6*) δ 174.63, 168.29, 159.94, 140.24, 134.57, 129.11, 127.97, 127.08 (d, J = 5.1 Hz), 126.13, 123.32 (d, J = 274.7 Hz), 123.55, 120.31, 118.56 (q, J = 31.3 Hz), 116.24, 115.43, 82.11 (d, J = 167.7 Hz), 69.23 (d, J = 19.2 Hz), 55.47, 52.71. HRMS (ESI) calcd for $C_{21}H_{17}F_4N_5O_3$ [M + H$^+$] 464.1346. Found [M + H$^+$] 464.1353.

4-(5-(4-(2-Fluoroethoxy)-3-(trifluoromethyl)phenyl)-1,2,4-oxadiazol-3-yl)benzaldehyde (13) [18]. To an oven-dried 100 mL round-bottom flask equipped with a stir bar was added CH_2Cl_2 (32 mL) and DMSO (1.7 g, 21.7 mmol). The reaction mixture was cooled to -78 °C and oxalyl chloride (1.87 g, 14.7 mmol) was added slowly under N$_2$ atmosphere. The reaction mixture was stirred for 30 minutes at which time **9e** (2.68 g, 7.0 mmol) was added. The reaction mixture was stirred for another 30 minutes at which time triethylamine (5.67 mL, 56.0 mmol) was added. The cooling bath was removed and the reaction was allowed to warm to room temperature over 2 h. The reaction mixture was concentrated *in vacuo* and partitioned between ethyl acetate and 1 M HCl. The layers were separated and the aqueous layer was re-extracted with ethyl acetate. The combined organic layers were washed with 1 M HCl, sat. NaHCO₃, brine, and dried over MgSO₄. After filtration and concentration *in vacuo*, a pale-yellow solid was obtained. (1.51 g, 76%).

***tert*-Butyl (1-(4-(5-(4-(2-fluoroethoxy)-3-(trifluoromethyl)phenyl)-1,2,4-oxadiazol-3-yl)benzyl)piperidin-4-yl)carba-mate (14)**. To a round-bottom flask equipped with a stir bar was added aldehyde **13** (380 mg, 1.0 mmol), amine (21 mg, 1.05 mmol), 1,2-dichloroethane (10 mL), sodium triacetoxyborohydride (318 mg, 1.5 mmol), and acetic acid (120 mg, 2.0 mmol). The reaction mixture was stirred overnight at room temperature. Then, the reaction was quenched with saturated NaHCO₃ aqueous and extracted with ethyl acetate (20 mL × 3). The combined ethyl acetate layer was washed with brine and dried over anhydrous MgSO₄. After filtration and concentration, the crude product was purified on a silica gel column to give white solid product (250 mg, 44%). MP: 147-149 °C. ^{1}H NMR (400 MHz, Acetone-*d6*) δ 8.39 – 8.32 (m, 2H, -*ArH*), 8.02 (d, J = 7.9 Hz, 2H, -*ArH*), 7.52 – 7.45 (m, 3H, -*ArH*), 5.83 (d, J = 6.7 Hz, 1H, -*ArH*), 4.90 – 4.83 (m, 1H, -*CH₂F*), 4.79 – 4.72 (m, 1H, -*CH₂F*), 4.61 – 4.56 (m, 1H, -*CH₂O-*), 4.55 – 4.49 (m, 1H, -*CH₂O-*), 3.51 (s, 2H, -*ArCH₂-*), 3.41 – 3.27 (m, 1H, -*CHNH-*), 2.83 – 2.75 (m, 2H, -*NCH₂-*), 2.12 – 1.97 (m, 2H, -*NCH₂-*), 1.83 – 1.75 (m, 2H, -*CH₂-*), 1.55 – 1.43 (m, 2H, -*CH₂-*), 1.34 (s, 9H, -*CH₃*). ^{13}C NMR (101 MHz, Acetone-*d6*) δ 174.29, 168.62, 159.90, 159.89, 155.00,

143.07, 133.74, 129.26, 127.11, 126.86 (q, J = 5.1 Hz), 125.33, 123.15 (d, J = 273.7 Hz), 119.17 (q, J = 31.3 Hz), 116.65, 114.43, 81.54 (d, J = 169.7 Hz), 77.51, 68.91 (d, J = 20.2 Hz), 62.18, 52.44, 47.89, 32.27, 27.75.

1-(4-(5-(4-(2-Fluoroethoxy)-3-(trifluoromethyl)phenyl)-1,2,4-oxadiazol-3-yl)benzyl)piperidin-4-amine dihydro-chloride (15). To a round-bottom flask equipped with a stir bar was added the Boc-protected amine **14** (90 mg, 0.16 mmol) and 2 mL of 4 M HCl in 1,4-dioxane. The reaction was stirred 4 h at room temperature, and the precipitate was filtered off, washed with ethyl ether to give a white solid. (51 mg, 59%). MP: 268-269 °C. ^{1}H NMR (400 MHz, DMSO-*d6*) δ 8.50 (s, 2H, *-NH₂*), 8.42 (d, J = 9.0 Hz, 1H, *-ArH*), 8.31 (s, 1H, *-ArH*), 8.14 (d, J = 7.9 Hz, 2H, *-ArH*), 7.85 (d, J = 7.4 Hz, 2H, *-ArH*), 7.58 (d, J = 8.8 Hz, 1H, *-ArH*), 4.90 – 4.81 (m, 1H, *-CH₂F*), 4.78 – 4.70 (m, 1H, *-CH₂F*), 4.63 – 4.56 (m, 1H, *-CH₂O-*), 4.55 – 4.49 (m, 1H, *-CH₂O-*), 4.36 (s, 2H, *-ArCH₂-*), 3.36 – 3.17 (m, 3H, *-N-CH₂-&-CHNH₂*), 3.16 – 3.00 (m, 2H, *-N-CH₂-*), 2.22 – 1.95 (m, 4H, *-CH₂CH-*). ^{13}C NMR (101 MHz, DMSO-*d6*) δ 174.75, 168.26, 159.99, 134.60, 133.60, 132.92, 127.81, 127.36, 127.10 (d, J = 5.1 Hz), 123.32 (d, J = 273.7 Hz), 118.58 (q, J = 31.3 Hz), 116.20, 115.52, 82.13 (d, J = 168.7 Hz), 69.27 (d, J = 18.2 Hz), 58.66, 49.97, 45.68, 27.21. HRMS (ESI) calcd for $C_{23}H_{24}F_4N_4O_2$ [M + H⁺] 465.1908. Found [M + H⁺] 465.1907.

General procedure for the synthesis of 16a-b. To a round-bottom flask equipped with a stir bar was added aldehyde **13** (1.0 eq), amine (1.5 eq), methanol (14 mL/mmol), and acetic acid (0.5 mL/mmol). The reaction mixture was stirred 1 h at which time sodium cyanoborohydride (1.0 eq) was added. The reaction mixture was stirred overnight and diluted with water. The precipitate was filtered off and washed with water to give an off-white solid product.

(4-(5-(4-(2-Fluoroethoxy)-3-(trifluoromethyl)phenyl)-1,2,4-oxadiazol-3-yl)benzyl)glycine (16a). Yield: 24%. MP: 175-176 °C. ^{1}H NMR (400 MHz, Acetone-*d6*) δ 8.49 – 8.35 (m, 2H, *-ArH*), 8.12 (d, J = 7.8 Hz, 2H, *-ArH*), 7.67 (d, J = 7.9 Hz, 2H, *-ArH*), 7.56 (d, J = 8.7 Hz, 1H, *-ArH*), 4.98 – 4.75 (m, 2H, *-CH₂F*), 4.71 – 4.54 (m, 2H, *-CH₂O-*), 3.98 (s, 2H, *-ArCH₂-*), 3.42 (s, 2H, *-CH₂COOH*). ^{13}C NMR (101 MHz, Acetone-*d6*) δ 174.36, 171.35, 168.62, 159.93, 143.12, 133.77, 129.47, 127.27, 126.88 (q, J = 5.1 Hz), 125.65, 123.15 (d, J = 273.7 Hz), 119.19 (q, J = 31.3 Hz), 116.66, 114.47, 81.56 (d, J = 168.7 Hz), 68.92 (d, J = 20.2 Hz), 57.26, 53.12. HRMS (ESI) calcd for $C_{20}H_{17}F_4N_3O_4$ [M + H⁺] 440.1228. Found [M + H⁺] 440.1210.

3-((4-(5-(4-(2-Fluoroethoxy)-3-(trifluoromethyl)phenyl)-1,2,4-oxadiazol-3-yl)benzyl)amino)propanoic acid (16b). Yield: 17%. MP: 198-200 °C. ^{1}H NMR (400 MHz, DMSO-*d6*) δ 8.49 – 8.37 (m, 1H, *-ArH*), 8.30 (s, 1H, *-ArH*), 8.17 – 7.98 (m, 2H, *-ArH*), 7.67 – 7.44 (m, 3H, *-ArH*), 4.92 – 4.70 (m, 2H, *-CH₂F*), 4.63 – 4.45 (m, 2H, *-CH₂O-*), 3.87 (s, 2H, *-ArCH₂-*), 2.87 – 2.71 (m, 2H, *-NHCH₂-*), 2.45 – 2.31 (m, 2H, *-CH₂COOH*). ^{13}C NMR (101 MHz, DMSO-*d6*) δ 174.48, 174.15, 168.53, 159.91, 143.50, 134.53, 129.37, 127.52, 127.05 (d, J = 5.1 Hz), 125.10, 123.33 (d, J = 5.1 Hz), 118.56 (d, J = 273.7 Hz), 116.31, 115.43, 82.12 (d, J = 168.7 Hz), 69.24 (d, J = 19.2 Hz), 51.89, 44.51, 34.00. HRMS (ESI) calcd for $C_{21}H_{19}F_4N_3O_4$ [M + H$^+$] 454.1384. Found [M + H$^+$] 454.1370.

*4.2.4. Synthesis of **21a-b***

General procedure for the synthesis of 18a-b. To a round-bottom flask equipped with a stir bar was added **17a-b** (1.0 eq), Boc₂O (1.1 eq), CH₂Cl₂ (10 mL/mmol), and triethylamine (1.5 eq). The reaction mixture was stirred at room temperature overnight. The reaction was concentrated *in vacuo* and partitioned between ethyl ether and 1 M HCl. The organic layer were separated, washed with saturated NaHCO₃, brine, dried over MgSO₄, and concentrated *in vacuo* to give a white crystalline solid.

tert-**Butyl (4-cyanobenzyl)carbamate (18a)**. Yield: 93%. MP: 114-116 °C. ^{1}H NMR (400 MHz, CDCl₃) δ 7.62 (d, J = 7.9 Hz, 2H, *-ArH*), 7.39 (d, J = 8.5 Hz, 2H, *-ArH*), 4.96 (s, 1H, *-NH-*), 4.37 (d, J = 5.9 Hz, 2H, *-CH₂-*), 1.46 (s, 9H, *-CH₃*).

tert-**Butyl (2-((4-cyanobenzyl)oxy)ethyl)carbamate (18b)**. Yield: 83%. MP: 100-102 °C. ^{1}H NMR (400 MHz, CDCl₃) δ 7.62 (d, J = 7.9 Hz, 2H, *-ArH*), 7.33 (d, J = 7.9 Hz, 2H, *-ArH*), 4.53 (s, 2H, *-ArCH₂-*), 3.80 – 3.65 (m, 2H, *-OCH₂-*), 3.49 – 3.30 (m, 2H, *-CH₂NH-*), 1.40 (s, 9H, *-CH₃*).

General procedure for the synthesis of 19a-b. To a round-bottom flask equipped with a stir bar was added **18a-b** (1.0 eq), hydroxylamine hydrochloride (2.0 eq), NaHCO₃ (4.0 eq), and methanol (10 mL/mmol). The reaction was refluxed and stirred in a pre-heated 75 °C oil-bath for 6 h. After cooling to room temperature, and the precipitate was filtered off and washed with methanol. The filtrate was concentrated *in vacuo* and further purified on a silica gel column.

23

tert-**Butyl** (*E*)-**(4-(*N'*-hydroxycarbamimidoyl)benzyl)carbamate** (**19a**). Yield: 65%. MP: 142-145 °C. ^{1}H NMR (400 MHz, DMSO-*d6*) δ 9.57 (s, 1H, *-OH*), 7.61 (d, *J* = 8.1 Hz, 2H, *-ArH*), 7.40 (t, *J* = 6.1 Hz, 1H, *-NHCO-*), 7.22 (d, *J* = 8.1 Hz, 2H, *-ArH*), 5.77 (s, 2H, *-NH₂*), 4.13 (d, *J* = 6.1 Hz, 2H, *-ArCH₂-*), 1.40 (s, 9H, *-CH₃*).

tert-**Butyl** (*E*)-**(2-((4-(*N'*-hydroxycarbamimidoyl)benzyl)oxy)ethyl)carbamate** (**19b**). Yield: 40%. MP: 138-140 °C. ^{1}H NMR (400 MHz, Acetone-*d6*) δ 8.87 (s, 1H, *-OH*), 7.69 (d, *J* = 7.7 Hz, 2H, *-ArH*), 7.28 (d, *J* = 8.1 Hz, 2H, *-ArH*), 5.45 (s, 2H, *-NH₂*), 4.54 (s, 2H, *-ArCH₂-*), 3.75 (s, 1H, *-NHCO-*), 3.68 – 3.59 (m, 2H, *-OCH₂-*), 3.40 – 3.24 (m, 2H, *-CH₂NH-*), 1.47 (s, 9H, *-CH₃*).

General procedure for the synthesis of 20a-b. To a round-bottom flask equipped with a stir bar was added acid **6** (1.0 eq), HOBt (0.2 eq), TBTU (1.0 eq), DMF (5 mL/mmol), and DIPEA (3.0 eq). The reaction mixture was stirred for 0.5 h before adding amidoxime **19a-b** (1.0 eq). The reaction mixture was stirred for 1 h at room temperature, then heated in a pre-heated 120 °C oil-bath. The reaction mixture was stirred for 4 h and monitored by TLC. After cooling, the reaction mixture was diluted with water and extracted with ethyl acetate. The ethyl acetate layer was washed with 1 M HCl, saturated brine, and dried over anhydrous MgSO₄. After filtration and concentration, the residue was purified on a silica gel column.

tert-**Butyl** **(4-(5-(4-(2-fluoroethoxy)-3-(trifluoromethyl)phenyl)-1,2,4-oxadiazol-3-yl)benzyl)carbamate** (**20a**). Yield: 56%. MP: 158-160 °C. ^{1}H NMR (400 MHz, DMSO-*d6*) δ 8.40 (d, *J* = 9.0 Hz, 1H, *-ArH*), 8.30 (s, 1H, *-ArH*), 8.03 (d, *J* = 8.0 Hz, 2H, *-ArH*), 7.58 – 7.47 (m, 2H, *-ArH&-NHCO*), 7.44 (d, *J* = 8.0 Hz, 2H, *-ArH*), 4.88 – 4.82 (m, 1H, *-CH₂F*), 4.76 – 4.70 (m, 1H, *-CH₂F*), 4.61 – 4.55 (m, 1H, *-CH₂O-*), 4.54 – 4.48 (m, 1H, *-CH₂O-*), 4.22 (d, *J* = 5.9 Hz, 2H, *-ArCH₂-*), 1.41 (s, 9H, *-CH₃*). ^{13}C NMR (101 MHz, DMSO-*d6*) δ 174.45, 168.52, 159.88, 156.27, 144.53, 134.49, 128.04, 127.54, 127.04 (q, *J* = 5.1 Hz), 123.33 (d, *J* = 273.7 Hz), 121.97, 118.56 (d, *J* = 30.3 Hz), 116.32, 115.40, 82.11 (d, *J* = 168.7 Hz), 78.39, 69.22 (d, *J* = 19.2 Hz), 43.66, 28.65.

tert-**Butyl** **(2-((4-(5-(4-(2-fluoroethoxy)-3-(trifluoromethyl)phenyl)-1,2,4-oxadiazol-3-yl)benzyl)oxy)ethyl)-carbamate** (**20b**). Yield: 42%. MP: 144-147 °C. ^{1}H NMR (400 MHz, CDCl₃) δ 8.47 (s, 1H, *-ArH*), 8.35 (d, *J* = 8.7 Hz, 1H, *-ArH*), 8.13 (d, *J* = 8.1 Hz, 2H, *-ArH*), 7.38 (d, *J* = 7.8 Hz, 2H, *-ArH*), 7.18 (d, *J* = 8.8 Hz, 1H, *-*

24

ArH), 4.92 – 4.86 (m, 1H, -*CH₂F*), 4.80 – 4.75 (m, 1H, -*CH₂F*), 4.56 (s, 2H, -*ArCH₂*-), 4.49 – 4.44 (m, 1H, -*CH₂O*-), 4.42 – 4.37 (m, 1H, -*CH₂OAr*-), 3.80 – 3.69 (m, 2H, -*OCH₂*-), 3.52 – 3.35 (m, 2H, -*CH₂NH*-), 1.46 (s, 9H, -*CH₃*).

General procedure for the synthesis of 21a-b. To a round-bottom flask equipped with a stir bar was added Boc-protected amine **20a-b** (1.0 eq), followed by 4 M HCl in 1,4-dioxane (20 eq). The reaction mixture was stirred for 2 h and concentrated *in vacuo*. The resulting residue was suspended in a mixture of ethanol and *tert*-butyl methyl ether (V/V, 3/1), and the resulting solid was filtered to give the white solid product.

(4-(5-(4-(2-Fluoroethoxy)-3-(trifluoromethyl)phenyl)-1,2,4-oxadiazol-3-yl)phenyl)methanamine hydrochloride (21a). Yield: 77%. MP: 276-277 °C. ^{1}H NMR (400 MHz, DMSO-*d6*) δ 8.71 (s, 2H, -*NH₂*), 8.39 (d, *J* = 8.4 Hz, 1H, -*ArH*), 8.29 (s, 1H, -*ArH*), 8.10 (d, *J* = 7.6 Hz, 2H, -*ArH*), 7.73 (d, *J* = 7.6 Hz, 2H, -*ArH*), 7.56 (d, *J* = 8.7 Hz, 1H, -*ArH*), 4.91 – 4.67 (m, 2H, -*CH₂F*), 4.62 – 4.46 (m, 2H, -*CH₂O*-), 4.12 (s, 2H, -*CH₂*-). ^{13}C NMR (101 MHz, DMSO-*d6*) δ 174.69, 168.31, 159.97, 138.18, 134.58, 130.23, 127.69, 127.10 (d, *J* = 5.1 Hz), 126.37, 123.34 (d, *J* = 273.7 Hz), 118.56 (d, *J* = 31.3 Hz), 116.24, 115.50, 82.13 (d, *J* = 168.7 Hz), 69.27 (d, *J* = 19.2 Hz), 42.24. HRMS (ESI) calcd for $C_{18}H_{15}F_4N_3O_2$ [M + H$^+$] 382.1173. Found [M + H$^+$] 382.1169.

2-((4-(5-(4-(2-Fluoroethoxy)-3-(trifluoromethyl)phenyl)-1,2,4-oxadiazol-3-yl)benzyl)oxy)ethan-1-amine (21b). Yield: 57%. MP: 266-267 °C. ^{1}H NMR (400 MHz, Acetone-*d6*) δ 8.47 – 8.35 (m, 2H, -*ArH*), 8.13 – 8.02 (m, 2H, -*ArH*), 7.65 – 7.49 (m, 3H, -*ArH*), 4.87 (d, *J* = 47.8 Hz, 2H, -*CH₂F*), 4.61 (d, *J* = 28.7 Hz, 2H, -*CH₂O*-), 3.89 (s, 2H, -*ArCH₂O*-), 3.71 – 3.57 (m, 2H, -*CH₂O*-), 2.78 – 2.66 (m, 2H, -*CH₂NH₂*). ^{13}C NMR (101 MHz, Acetone-*d6*) δ 174.27, 168.67, 159.90, 145.17, 133.73, 128.82, 128.49, 127.16, 127.08, 126.86 (q, *J* = 5.1 Hz), 123.15 (d, *J* = 273.7 Hz), 119.18 (q, *J* = 31.3 Hz), 114.43, 81.54 (d, *J* = 169.7 Hz), 68.91 (d, *J* = 31.3 Hz), 60.86, 52.94, 51.25. HRMS (ESI) calcd for $C_{20}H_{19}F_4N_3O_3$ [M + H$^+$] 426.1435. Found [M + H$^+$] 426.1432.

4.3. In vitro S1PRs binding assay

[^{32}P]S1P was firstly prepared by incubating sphingosine and [γ-^{32}P]ATP with sphingosine kinase 1 as we previously reported [20]. [^{32}P]S1P was dissolved in DMSO, and then diluted in the assay buffer (50 mM HEPES-Na with 5 mM MgCl₂, 1 mM CaCl₂, and 0.5% fatty acid-free bovine serum albumin, pH = 7.5).

Compounds were dissolved in DMSO and diluted to different concentrations with assay buffer, followed by adding commercial cell membranes expressing recombinant human S1PRs (1, 2, 3, 4, and 5) in the assay buffer at room temperature in 96-well plate. $[^{32}P]$S1P solution was then added to give a final volume of 150 μL containing 0.1 nM of $[^{32}P]$S1P and 1 μg of membrane protein per well. Competitive binding was performed for 60 min at room temperature and terminated by collecting the membranes onto 96-well glass fiber (GF/B) filtration plates (Millipore, Billerica, MA). Each filter was washed with 200 μL of assay buffer for five times. The filter bound radionuclide was measured by a Beckman LS3801 scintillation counter using Cherenkov counting. The reported IC$_{50}$ values were calculated using the 4 parameter equation, least-square non-linear regression curve-fit, with GraphPad Prism software (GraphPad Software, Inc). Each assay was repeated at least three times with duplicate wells for each compound; the reported values (mean $\pm$ SD, nM) are calculated from the average of all assays. Assays for compounds which showed no activity (IC$_{50}$ > 1000 nM) were only repeated twice.

4.4. Radiochemistry

4.4.1. Synthesis of precursor 25

4-(3-(4-(Hydroxymethyl)phenyl)-1,2,4-oxadiazol-5-yl)-2-(trifluoromethyl)phenol (22) [18]. To a round-bottom flask equipped with a stir bar was added 4-hydroxy-3-(trifluoromethyl)benzoic acid (1.96 g, 9.51 mmol), HOBt (0.26g, 1.90 mmol), TBTU (3.05 g, 9.51 mmol), DMF (20 mL), and DIPEA (3.69 g, 28.5 mmol). The reaction mixture was stirred for 0.5 h before adding **8e** (1.58 g, 9.51 mmol). The reaction mixture was stirred for 1 h at room temperature and refluxed in a pre-heated 120 °C oil-bath. The reaction mixture was stirred for 4 h and monitored by TLC. After cooling, the reaction mixture was diluted with water and extracted with ethyl acetate. The ethyl acetate layer was washed with 1 M HCl, saturated brine, and dried over anhydrous MgSO$_4$. After filtration and concentration, the residue was purified on a silica gel column. (1.43 g, 45%)

4-(3-(4-(Azidomethyl)phenyl)-1,2,4-oxadiazol-5-yl)-2-(trifluoromethyl)phenol (23). To a round-bottom flask equipped with a stir bar was added **22** (1.39 g, 4.13 mmol), diphenyl phosphoryl azide (1.37 g, 4.96 mmol), and toluene (10.0 mL). The mixture was cooled to 0 °C before adding 1,8-Diazabicyclo[5.4.0]undec-7-ene (0.76,

4.96 mmol) dropwise. The reaction was warmed to room temperature slowly and stirred overnight. Then, the reaction mixture was diluted with water and extracted with ethyl acetate. The ethyl acetate layer was washed with 1 M HCl, saturated brine and dried over anhydrous $MgSO_4$. After filtration and concentration, the residue was purified on a silica gel column to give yellow solid (815 mg, 55%). MP: 158-161°C. ^{1}H NMR (400 MHz, $CDCl_3$) δ 8.41 (s, 1H, -*ArH*), 8.22 (d, *J* = 8.5 Hz, 1H, -*ArH*), 8.17 (d, *J* = 7.8 Hz, 2H, -*ArH*), 7.47 (d, *J* = 7.9 Hz, 2H, -*ArH*), 7.09 (d, *J* = 8.6 Hz, 1H, -*ArH*), 4.44 (s, 2H, -*CH₂*-).

2-(4-(3-(4-(Azidomethyl)phenyl)-1,2,4-oxadiazol-5-yl)-2-(trifluoromethyl)phenoxy)ethyl 4-methylbenzene-sulfonate (24). To a round-bottom flask equipped with a stir bar was added **23** (500 mg, 1.38 mmol), ethylene ditosylate (767 mg, 2.07 mmol), K_2CO_3 (953 mg, 6.90 mmol), and CH_3CN (10.0 mL). The reaction mixture was refluxed in a pre-heated 90 °C oil-bath for 12 h. After cooling, the reaction mixture was diluted with water and extracted with ethyl acetate. The ethyl acetate layer was washed with saturated brine and dried over anhydrous $MgSO_4$. After filtration and concentration, the residue was purified on a silica gel column to give white solid (300 mg, 39%). MP: 169-170 °C. ^{1}H NMR (400 MHz, $CDCl_3$) δ 8.44 (s, 1H, -*ArH*), 8.33 (d, *J* = 8.7 Hz, 1H, -*ArH*), 8.19 (d, *J* = 8.2 Hz, 2H, -*ArH*), 7.81 (d, *J* = 8.3 Hz, 2H, -*ArH*), 7.48 (d, *J* = 8.1 Hz, 2H, -*ArH*), 7.38 – 7.32 (m, 2H, -*ArH*), 7.10 (d, *J* = 8.7 Hz, 1H, -*ArH*), 4.45 (s, 2H, -*ArCH₂*-), 4.43 – 4.38 (m, 4H, -*OCH₂CH₂O*-), 2.45 (s, 3H, -*CH₃*).

2-(4-(3-(4-((4-(hydroxymethyl)-1*H*-1,2,3-triazol-1-yl)methyl)phenyl)-1,2,4-oxadiazol-5-yl)-2-(trifluorome-thyl)phenoxy)ethyl 4-methylbenzenesulfonate (25). To a round-bottom flask equipped with a stir bar was added azide **24** (243 mg, 0.43 mmol) and THF (2.0 mL). Once the azide was dissolved, water (1.1 mL) was added followed by 3-(methoxymethoxy)prop-1-yne (46 mg, 0.46 mmol), sodium ascorbate (8.5 mg, 0.043 mmol), and copper sulfate pentahydrate (6.4 mg, 0.026 mmol). The reaction mixture was stirred for 4 h and monitored by TLC. Then, the reaction mixture was diluted with water and extracted with ethyl acetate. The ethyl acetate layer was washed with saturated brine and dried over anhydrous $MgSO_4$. After filtration and concentration, a white solid was obtained (100 mg, 35%). MP: 168-171°C. ^{1}H NMR (400 MHz, CD_3OD) δ 8.35 – 8.29 (m, 2H, -*ArH*), 8.11 (d, *J* = 7.2 Hz, 2H, -*ArH*), 8.02 (s, 1H, -*ArH*), 7.74 (d, *J* = 7.3 Hz, 2H, -*ArH*), 7.45 (d, *J* = 7.5 Hz, 2H, -*ArH*), 7.36 (d, *J* = 8.0 Hz, 2H, -*ArH*), 7.31 (d, *J* = 8.4 Hz, 1H, -*ArH*), 5.67 (s, 2H, -*ArCH₂*-),

4.65 – 4.61 (m, 4H, *-CH$_2$OCH$_2$O-*), 4.43 – 4.34 (m, 4H, *-OCH$_2$CH$_2$O-*), 3.27 (s, 3H, *-OCH$_3$*), 2.37 (s, 3H, *-ArCH$_3$*).

4.4.2. Radiosynthesis of [^{18}F]**12b**

[^{18}F]KF (~7.4 GBq) aqueous was added to a vial containing Kryptofix 222 (~6 mg), and dried by azeotropic evaporation with CH$_3$CN (3 x 1 mL) under N$_2$ flow at 110 °C. To the reaction vial was added precursor **25** (2 mg) as a solution in CH$_3$CN (300 μL). The reaction was placed in a 110 °C oil-bath for 15 min. The reaction was removed from the oil-bath, at which time 6 M HCl (150 µL) was added. The reaction mixture was heated in a 110 °C oil-bath for another 5 min. The reaction was removed from the oil-bath and quenched with 6 M NaOH (150 µL) and diluted with 2.4 mL of the HPLC mobile phase (45% CH$_3$CN in 0.1 M ammonium formate buffer, pH = 4.5). The mixture was passed through a Sep-Pak® Alumina N Cartridge (Part No. WAT020510) and injected onto the semi-preparation HPLC column (Agilent SB-C18 250 x 9.6 mm, 5 μm, UV = 254 nm, 4.0 mL/min). The retention time of [^{18}F]**12b** is around 19-22 min. The HPLC fraction was collected into a water bottle with 60 mL of water and then trapped on a Sep-Pak® C-18 Cartridge (Part No. WAT020515). The activity (~740 MBq) was washed out with 0.6 mL of ethanol and 5.4 mL of 0.9% saline. After sterile filtration into a glass vial, the [^{18}F]**12b** was ready for quality control (QC) analysis and animal studies. An aliquot of sample was injected onto an analytical HPLC to determine the concentration of tracer. Meanwhile, the tracer was authenticated by co-injected with non-radiolabeled standard **12b** sample solution. The HPLC condition are as follows: Agilent Zorbax SB-C18 column (250 × 4.6 mm); UV absorbance at 254 nM; the mobile phase is consisted of 45% CH$_3$CN in 0.1 M ammonium formate buffer, pH = 4.5; the flow rate is 1.0 mL/min; the retention time of [^{18}F]**12b** is 5.7 min.

4.5. Ex vivo autoradiography study

An adult male SD rat (~450 g, Charles River) was injected with [^{18}F]**12b** (~55 MBq) via the tail vein under 2–3% isoflurane/oxygen anesthesia and euthanized at 60 min post-injection. The brain was immediately removed and snap-frozen over dry ice followed by sectioning at 100 µm and mounting on glass slides. Frozen slides were directly exposed to a BAS storage phosphor screen film (BAS-IP-MS-2025) in an imaging cassette (Fuji Photo

Film Co., Tokyo, Japan) for 12 h at -80 °C under the dark. The distribution of radioactivity was visualized by a Fuji Bio-Imaging Analyzer FLA-7000 (Fuji Photo Film Co., Tokyo, Japan).

4.6. In vitro autoradiography study in LPS-treated mice

Adult male C57BL/6 mice (20-25 g, Charles River Inc., Frederick, MD) were used to generate LPS-induced neuroinflammation murine model. The mice (n = 2) received an intraperitoneal injection of LPS from E. coli 055:B5 (Sigma-Aldrich, St. Louis, MO, USA) in saline (3 mg/mL) at dose of 15 mg/kg (5 mL/kg) and then euthanized at 24 h post-injection. Mouse brains were collected and cut into 20 μm sequential sections using a Microm cryotome and mounted on glass slides. For the control study, the slides were incubated with ~6 nM of [^{18}F]**12b** at room temperature for 60 min. For the blocking studies, slides were incubated with [^{18}F]**12b** in the presence of 10 μM of SEW2871 at room temperature for 60 min. Following the incubation, the brain sections were washed and exposed to the Storage Phosphor Screen in an imaging cassette overnight in -20° C at dark for 12 h. The distribution of radioactivity were visualized by a Fuji Bio-Imaging Analyzer FLA-7000 (Fuji Photo Film, Tokyo, Japan). Photo-stimulated luminescence (PSL) from the brain slices was quantified using Multi Gauge v3.0 software (Fuji Photo Film Co., Tokyo, Japan). Data were background-corrected, and expressed as photo-stimulated luminescence signals per square millimeter (PSL/mm^2).

4.7. Biodistribution study

A solution of [^{18}F]**12b** (~2.2 MBq/100 μL) in 10% ethanol in 0.9% saline was injected via the tail vein into adult female Lewis rats (n = 16, 120-140 g, Charles River) under 2-3% isoflurane/oxygen anesthesia. The rats were euthanized under anesthesia at 5, 30, 60, and 120 min post-injection (n = 4 for each group). The whole brains were quickly harvested and dissected into regions of cerebellum, brain stem, cortex, striatum, thalamus, and hippocampus, the remainder of the brain was also collected to determine the total brain uptake. Organs of blood, heart, lung, muscle, fat, pancreas, spleen, kidney, liver, thymus, and bone were also dissected and collected for counting. All the samples were counted with a dilution of the injectate on an automated well counter (Beckman Gamma 8000 well counter). Tissues were weighed and the uptake was reported as background and decay-corrected percent injected dose per gram (% ID/g).

Acknowledgements

Abbreviations

S1PR1   Sphingosine-1-phosphate receptor 1

MS   Multiple sclerosis

FDA   Food and Drug Administration

PET   Positron emission tomography

LPS   Lipopolysaccharides

CNS   Central nervous system

SAR   Structure activity relationship

BBB   Blood-brain barrier

RT   Room temperature

TBTU   *O*-(Benzotriazol-1-yl)-*N,N,N',N'*-tetramethyluronium tetrafluoroborate

HOBt   Hydroxybenzotriazole hydrate

DBU   1,8-Diazabicyclo[5.4.0]undec-7-ene

DIPEA   *N,N*-Diisopropylethylamine

DPPA   Diphenyl phosphoryl azide

Boc   *tert*-Butyloxycarbonyl

MW   Molecular weight

ClogP   Calculated partition coefficient

TPSA   Topological polar surface area

HBD   Hydrogen bond donor

HPLC   High-performance liquid chromatography

SD   Sprague-Dawley

TLC   Thin-layer chromatography

References

[1] G.T. Kunkel, M. MacEyka, S. Milstien, S. Spiegel, Targeting the sphingosine-1-phosphate axis in cancer, inflammation and beyond, Nat. Rev. Drug. Discov. 12 (2013) 688-702.

[2] J. Rivera, R.L. Proia, A. Olivera, The alliance of sphingosine-1-phosphate and its receptors in immunity, Nat. Rev. Immunol. 8 (2008) 753-763.

[3] C.S. Garris, V.A. Blaho, T. Hla, M.H. Han, Sphingosine-1-phosphate receptor 1 signalling in T cells: trafficking and beyond, Immunology 142 (2014) 347-353.

[4] D.C. Montrose, E.J. Scherl, B.P. Bosworth, X.K. Zhou, B. Jung, A.J. Dannenberg, T. Hla, $S1P_1$ localizes to the colonic vasculature in ulcerative colitis and maintains blood vessel integrity, J. Lipid. Res. 54 (2013) 843-851.

[5] J.R. Teijaro, K.B. Walsh, S. Cahalan, D.M. Fremgen, E. Roberts, F. Scott, E. Martinborough, R. Peach, M.B. Oldstone, H. Rosen, Endothelial cells are central orchestrators of cytokine amplification during influenza virus infection, Cell 146 (2011) 980-991.

[6] H. Takeshita, M. Kitano, T. Iwasaki, S. Kitano, S. Tsunemi, C. Sato, M. Sekiguchi, N. Azuma, K. Miyazawa, T. Hla, H. Sano, Sphingosine 1-phosphate (S1P)/S1P receptor 1 signaling regulates receptor activator of NF-κB ligand (RANKL) expression in rheumatoid arthritis, Biochem. Biophys. Res. Commun. 419 (2012) 154-159.

[7] T. Karuppuchamy, E.H. Behrens, P. Gonzalez-Cabrera, G. Sarkisyan, L. Gima, J.D. Boyer, G. Bamias, P. Jedlicka, M. Veny, D. Clark, R. Peach, F. Scott, H. Rosen, J. Rivera-Nieves, Sphingosine-1-phosphate receptor-1 ($S1P_1$) is expressed by lymphocytes, dendritic cells, and endothelium and modulated during inflammatory bowel disease, Mucosal Immunol. 10 (2017) 162-171.

[8] J.R. Nofer, M. Bot, M. Brodde, P.J. Taylor, P. Salm, V. Brinkmann, T. van Berkel, G. Assmann, E.A. Biessen, FTY720, a synthetic sphingosine 1 phosphate analogue, inhibits development of atherosclerosis in low-density lipoprotein receptor-deficient mice, Circulation 115 (2007) 501-508.

[9] H. Liu, H. Jin, J. Han, X. Yue, H. Yang, M.A. Zayed, R.J. Gropler, Z. Tu, Upregulated sphingosine 1-phosphate receptor 1 expression in human and murine atherosclerotic plaques, Mol. Imaging Biol. (2017). http://doi.org/10.1007/s11307-11017-11141-11303.

[10] V. Brinkmann, A. Billich, T. Baumruker, P. Heining, R. Schmouder, G. Francis, S. Aradhye, P. Burtin, Fingolimod (FTY720): discovery and development of an oral drug to treat multiple sclerosis, Nat. Rev. Drug. Discov. 9 (2010) 883-897.

[11] J. Chun, H.-P. Hartung, Mechanism of action of oral Fingolimod (FTY720) in multiple sclerosis, Clin. Neuropharmacol. 33 (2010) 91-101.

[12] B.K. Das, Development of Positron Emission Tomography (PET): A Historical Perspective, in: B.K. Das (Ed.) Positron Emission Tomography: A Guide for Clinicians, Springer India, New Delhi, 2015, pp. 7-11.

[13] H. Liu, H. Jin, X. Yue, Z. Luo, C. Liu, A.J. Rosenberg, Z. Tu, PET imaging study of S1PR1 expression in a rat model of multiple sclerosis, Mol. Imaging Biol. 18 (2016) 724-732.

[14] H. Jin, H. Yang, H. Liu, Y. Zhang, X. Zhang, A.J. Rosenberg, Y. Liu, S.E. Lapi, Z. Tu, A promising carbon-11-labeled sphingosine-1-phosphate receptor 1-specific PET tracer for imaging vascular injury, J. Nucl. Cardiol. 24 (2017) 558-570.

[15] H. Liu, H. Jin, X. Yue, J. Han, P. Baum, D.R. Abendschein, Z. Tu, PET study of sphingosine-1-phosphate receptor 1 expression in response to vascular inflammation in a rat model of carotid injury, Mol. Imaging 16 (2017) 1-7.

[16] V.P. Prasad, S. Wagner, P. Keul, S. Hermann, B. Levkau, M. Schäfers, G. Haufe, Synthesis of fluorinated analogues of sphingosine-1-phosphate antagonists as potential radiotracers for molecular imaging using positron emission tomography, Bioorg. Med. Chem. 22 (2014) 5168-5181.

[17] R.S. Shaikh, S.S. Schilson, S. Wagner, S. Hermann, P. Keul, B. Levkau, M. Schäfers, G. Haufe, Synthesis and evaluation of fluorinated fingolimod (FTY720) analogues for sphingosine-1-phosphate receptor molecular imaging by positron emission tomography, J. Med. Chem. 58 (2015) 3471-3484.

[18] A.J. Rosenberg, H. Liu, H. Jin, X. Yue, S. Riley, S.J. Brown, Z. Tu, Design, synthesis, and *in vitro* and *in vivo* evaluation of an ^{18}F-labeled sphingosine 1-phosphate receptor 1 (S1P1) PET tracer, J. Med. Chem. 59 (2016) 6201-6220.

[19] J.L. Gilmore, J.E. Sheppeck, S.H. Watterson, L. Haque, P. Mukhopadhyay, A.J. Tebben, M.A. Galella, D.R. Shen, M. Yarde, M.E. Cvijic, V. Borowski, K. Gillooly, T. Taylor, K.W. McIntyre, B. Warrack, P.C. Levesque, J.P. Li, G. Cornelius, C. D'Arienzo, A. Marino, P. Balimane, L. Salter-Cid, J.C. Barrish, W.J. Pitts, P.H. Carter, J. Xie, A.J. Dyckman, Discovery and structure–activity relationship (SAR) of a series of ethanolamine-based direct-acting agonists of sphingosine-1-phosphate (S1P1), J. Med. Chem. 59 (2016) 6248-6264.

[20] A.J. Rosenberg, H. Liu, Z. Tu, A practical process for the preparation of [^{32}P]S1P and binding assay for S1P receptor ligands, Appl. Radiat. Isot. 102 (2015) 5-9.

[21] A.K. Ghose, T. Herbertz, R.L. Hudkins, B.D. Dorsey, J.P. Mallamo, Knowledge-based, central nervous system (CNS) lead selection and lead optimization for CNS drug discovery, ACS Chem. Neurosci. 3 (2012) 50-68.

[22] T.T. Wager, X. Hou, P.R. Verhoest, A. Villalobos, Central nervous system multiparameter optimization desirability: application in drug discovery, ACS Chem. Neurosci. 7 (2016) 767-775.

[23] T.T. Wager, Moving beyond rules: the development of a central nervous system multiparameter optimization (CNS MPO) approach to enable alignment of druglike properties, ACS Chem. Neurosci. 1 (2010) 435-449.

[24] Z. Rankovic, CNS drug design: balancing physicochemical properties for optimal brain exposure, J Med Chem 58 (2015) 2584-2608.

[25] Z. Rankovic, CNS physicochemical property space shaped by a diverse set of molecules with experimentally determined exposure in the mouse brain, J. Med. Chem. 60 (2017) 5943-5954.

[26] R.E. Toman, S. Spiegel, Lysophospholipid receptors in the nervous system, Neurochem. Res. 27 (2002) 619-627.

[27] H. Ohuchi, A. Hamada, H. Matsuda, A. Takagi, M. Tanaka, J. Aoki, H. Arai, S. Noji, Expression patterns of the lysophospholipid receptor genes during mouse early development, Dev. Dyn. 237 (2008) 3280-3294.

[28] H. Nishimura, T. Akiyama, I. Irei, S. Hamazaki, Y. Sadahira, Cellular localization of sphingosine-1-phosphate receptor 1 expression in the human central nervous system, J. Histochem. Cytochem. 58 (2010) 847-856.

[29] M. Kono, E.G. Conlon, S.Y. Lux, K. Yanagida, T. Hla, R.L. Proia, Bioluminescence imaging of G protein-coupled receptor activation in living mice, Nat. Commun. 8 (2017) 1163.

[30] J. Dong, H. Wang, G. Wu, J. Zhao, L. Zhang, L. Zuo, W. Zhu, J. Gong, Y. Li, L. Gu, J. Li, Oral treatment with SEW2871, a sphingosine-1-phosphate type 1 receptor agonist, ameliorates experimental colitis in interleukin-10 gene deficient mice, Clin. Exp. Immunol. 177 (2014) 94-101.

- Compound **12b** showed high potency (9.7 nM) and selectivity toward S1PR1 over S1PR2-5 (> 100-fold).

- [^{18}F]**12b** was radiosynthesized with good radiochemical yield, high purity, and specific activity.

- [^{18}F]**12b** was able to cross the blood-brain barrier with high brain uptake.

- *In vitro* autoradiography study in LPS-induced neuroinflammation murine model indicated that [^{18}F]**12b** has specific binding toward S1PR1.